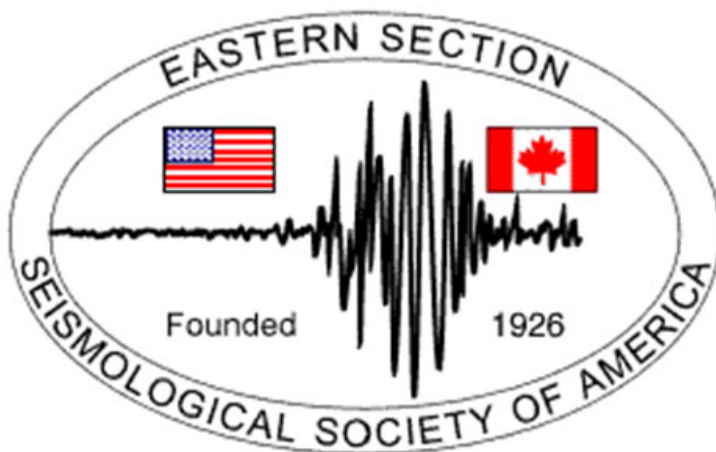


# ES-SSA 2025 Annual Meeting: Celebrating 100 Years of the ES-SSA

October 27–28, 2025, St. Louis, MO, USA



Co-chairs: R. H. Herrmann, L. Warren, and L. Zhu  
Supporting Staff: Gina Hostetler, Kyle Macy, Amit Bera, Elwin Chen  
Md Ahsan Habib, Mike Andramuno, and Muntadher Al-Kaabi  
Saint Louis University

Special Thanks to the Meeting Sponsors:



## Important Notes

- Your meeting badge gives you access to the meeting venue and also serve as tickets to the reception icebreaker and banquet.
- The poster size is 38"×50" maximum. Please put your poster on your assigned board by 8:30am and remove it after 5:00pm of the presentation day.
- The oral presentation PPT size is 16:9, please email us your PPT or upload it to the room computer at least 15 min before your session starting time.
- Parking On-campus parking is available for \$6/day in the Laclede Garage (3602 Laclede Ave) or Olive garage (3338 Olive St).
- There are several cafeterias to grab a bite in BSC. There are also restaurants in walking distances around the campus on the Grand Blvd, Lindell Ave, and Laclede Ave.
- More up-to-date information can be found at [www.eas.slu.edu/eqc/ESSA25](http://www.eas.slu.edu/eqc/ESSA25).
- Need help? email lupei.zhu@slu.edu.



Figure 1: A campus map of SLU with the two visitor parking garages and three meeting venue buildings labeled



## Meeting At A Glance

Date	Times	Events	Location
Sunday Oct. 26	14:00–18:00	Pickup meeting materials and on-site registration	BSC 172
	13:30–16:00	Computer Programs in Seismology Workshop	O’Neil Hall 206
	18:00–20:00	Icebreaker Reception	DuBourg Hall 204
	20:00–21:00	ES-SSA Board Meeting (closed door)	O’Neil Hall 206
Monday Oct. 27	08:00–16:00	Pickup meeting materials and on-site registration	BSC 172
	08:15–08:30	Opening Remarks	BSC 173
	08:30–09:45	Session S1 (Oral): CENA	BSC 173
	09:45–09:55	Group Photo	Outside BSC
	09:55–10:45	Session S2 (Poster): CENA	BSC 172
	10:45–12:00	Session S3 (Oral): CENA	BSC 173
	12:00–13:30	Lunch Break	On your own
	13:30–14:45	Session S4 (Oral): General	BSC 173
	14:45–15:45	Session S5 (Poster): General	BSC 172
	15:45–17:00	Session S6 (Oral): General	BSC 173
Tuesday Oct. 28	18:00–20:00	Banquet and JSA Award	BSC 171
	08:30–09:15	Session S7 (Oral): Gulf & Atlantic Coast	BSC 173
	09:15–10:15	Session S8 (Poster): General	BSC 172
	10:15–11:45	Session S9 (Oral): Induced & Exotic Seismicity	BSC 173
	11:45–11:50	Raspberry Shake Raffle	BSC 173
	11:50–12:00	Student Presentation Awards	BSC 173
	12:00–13:30	Lunch Break	On your own
	13:30–14:00	ES-SSA Business Meeting	BSC 173
	14:15–16:30	Session SM: Macelwane Lectures	BSC 173
	16:30–16:45	Closing Remarks	BSC 173

A campus map with the BSC, O’Neil, and DuBourg Halls labeled is shown on page 1.

## 1 Monday, October 27

(Underline indicates student **presenter**)

**Session S1 (Oral): Advances in Understanding Structures and Stresses in Central and Eastern North America Seismic Zones. Session Chair: Seth Carpenter**

**08:30–08:45 S1-1** New Madrid Seismic Zone Seismicity Patterns over Time and Space. **Langston, C.** and C. A. Powell (University of Memphis)

**08:45–09:00 S1-2** Solid earth tides have a stronger effect than seasonal water loading on earthquake modulation in the New Madrid Seismic Zone. **Walter, J.**<sup>1</sup>, H. DeShon<sup>2</sup>, P. Neupane<sup>2</sup> (1: Oklahoma Geological Survey; 2: Southern Methodist University)

**09:00–09:15 S1-3** New Velocity and Fault Structure Analysis of the New Madrid Seismic Zone. **Powell, C.**, C.A. Langston (University of Memphis)

**09:15–09:30 S1-4** Gravity Models Suggest Fluid Processes Associated with Mississippi Embay-

ment Conductive and Low Seismic Velocity Anomalies in the Crust and Mantle. **Cramer, C.** (CERI, University of Memphis)

**09:30–09:45 S1-5** Beyond New Madrid: Seismicity of Missouri. **Woods, M.**<sup>1</sup>, H.A.A. Ghalib<sup>2</sup>, and Y. Wang<sup>2</sup> (1: AFTAC; 2: EMR Solutions & Technology)

**Session S2 (Posters): 09:45–10:45 Advances in Understanding Structures and Stresses in Central and Eastern North America Seismic Zones**

**S2-1** A Seismic Array over the SW Arm of the NMSZ. **Bazargan, S.**<sup>1</sup>, S. Horton<sup>1</sup>, C. Langston<sup>1</sup>, S. Ausbrooks<sup>2</sup> (1: CERI, University of Memphis; 2: Office of the State Geologist of Arkansas)

**S2-2** Resistivity Structure of the Alabama-Oklahoma Lineament and the Mississippi Embayment. K. Sarker and **Cramer, C.** (CERI, University of Memphis)

**S2-3** Statistical Properties of Early Aftershocks Following Moderate-size Earthquakes in the Central and Eastern United States. **Ding, C.**<sup>1</sup>, Z. Peng<sup>1</sup>, J. Zhuang<sup>2</sup>, and X. Si<sup>1</sup> (1: Georgia Tech; 2: Institute of Statistical Mathematics)

**S2-4** Fracture-Mediated Water Level Changes at a Groundwater Well in Virginia (2008-2025). **Gribbins, J.**<sup>1</sup>, J. Maynard<sup>2</sup>, S. Thompson<sup>1</sup>, R.J. Hung<sup>1</sup>, N.G. Randolph-Flagg<sup>1</sup> (1: University of Kentucky; 2: Virginia Department of Environmental Quality)

**S2-5** A New Joint Inversion Method for Constructing High-Resolution 1-D Crustal Seismic Velocity Structures. **Habib, M.** and L. Zhu (Saint Louis University)

**S2-6** Refining GPS Time Series Analysis for Strain Estimation in the New Madrid Seismic Zone. **Heydarizadeh Shali, H.**<sup>1</sup>, Robert Smalley<sup>1</sup>, Demian Gomez<sup>2</sup> (1: CERI, University of Memphis; 2: Ohio States University)

**S2-7** Fault activity in CEUS seismic zones: Past focal planes to long-term slip potential. **Levandowski, W.** (Tetra Tech, Inc.)

**S2-8** Waveform Analysis of Three Earthquakes in 2021, Baltimore County, MD. **McLaughlin, K.** (Self)

**S2-9** Characterization of the 2024 Mw 4.8 Tewksbury, NJ Earthquake Fault Plane Geometry using Relocated Aftershocks. **Petschek, E.**, J. E. Ebel (Boston College)

**S2-10** Probing Crustal Structure Across the Central United States Using P-to-S Converted Receiver Functions and Teleseismic P-wave Coda Autocorrelograms. **Soni, Y.**<sup>1</sup> and N. Seth Carpenter<sup>2</sup> (1: Baylor University; 2: Kentucky Geological Survey, University of Kentucky)

**S2-11** Re-analyzing Eastern North America Seismic Archives to Study Seismogenic Processes and Improve Seismic Monitoring. **Waldhauser, F.**<sup>1</sup>, E. Beauché<sup>1</sup>, W.-Y. Kim<sup>1</sup>, D. Schaff<sup>1</sup>, K. Wang<sup>2</sup>, W. Zhu<sup>3</sup> (1: Columbia University; 2: Chinese Academy of Sciences; 3: UC Berkeley)

**Session S3 (Oral): Advances in Understanding Structures and Stresses in Central and Eastern North America Seismic Zones. Session Chair: Chuck Langston**

**10:45–11:00 S3-1** Unveiling Shear Velocity Anomalies in the Central Midcontinent of the United States through High-Resolution Joint Inversion: Links to Failed Rifting, Crustal Underplating, and Trans-Crustal Faulting. **Xiao, H.**<sup>1</sup>, S. Marshak<sup>2</sup>, X. Song<sup>3</sup> (1: University of Oklahoma; 2: University of Illinois Urbana-Champaign; 3: Peking University)

**11:00–11:15 S3-2** Joint inversion of receiver functions and surface-wave dispersion in the Eastern Tennessee Seismic Zone. **Julià, J.**<sup>1</sup>, V. Levin<sup>1</sup>, C. Chai<sup>2</sup>, M. Maceira<sup>3</sup> (1: CERI, University of Memphis; 2: Oak Ridge National Lab; 3: ORNL)

- 11:15–11:30 S3-3** Mid-crustal earthquakes in eastern Tennessee occur within a volume of layered sheared rock. **Levin, V.**, Jordi Julià Casas, Anuradhapura Mahanama (CERI, University of Memphis)
- 11:30–11:45 S3-4** Toward Defining the Northern Boundary of the Eastern Tennessee Seismic Zone. **N. Carpenter, S.**, C. A. Powell, W. Levandowski, J. B. Hickman, J. P. Schmidt, Z. Peng, M. C. Chapman (Kentucky Geological Survey, University of Kentucky)
- 11:45–12:00 S3-5** Lithologic controls on the Mw5.1 Sparta, NC seismic cycle - microgravity and crustal stress constraints. **Levandowski, W.** (Tetra Tech, Inc.)

#### Session S4 (Oral): General. Session Chair: Xiawei Chen

- 13:30–13:45 S4-1** Why are foreshocks rate in nature?: A laboratory perspective on accelerating fault slip and earthquake nucleation. **Goebel, T.**<sup>1</sup>, V. Schuster<sup>2</sup>, G. Kwiatek<sup>2</sup>, K. Pandey<sup>3</sup>, and G. Dresen<sup>2</sup> (1: University of Memphis; 2: GFZ-Potsdam; 3: UES)
- 13:45–14:00 S4-2** Adventures in improving earthquake depth estimates, Texas. **DeShon, H.**, Y. Seldon, and J. Sharma (Southern Methodist University)
- 14:00–14:15 S4-3** DYNAMIC TRIGGERING OF EARTHQUAKES IN COSTA RICA. **Hajaji, S.**<sup>1</sup> and E. Chaves<sup>2</sup> (1: Georgia Tech; 2: OVSICORI-UNA)
- 14:15–14:30 S4-4** A Spatial Forecast of Some  $M_w \geq 6.5$  Earthquakes in California and Nevada. **Ebel, J.** (Boston College)
- 14:30–14:45 S4-5** Evidence of lithospheric delamination below the North American midcontinent that ended subsidence in cratonic basins. **Yang, X.**<sup>1</sup>, L. Peng<sup>2</sup>, A. L. Stevens Goddard<sup>3</sup>, L. Liu<sup>4</sup> (1: Purdue University; 2: University of Illinois Urbana-Champaign; 3: Indiana University; 4: IGG, Chinese Academy of Sciences)

#### Session S5 (Posters): 14:45–15:45 General

- S5-1** Site-Specific Seismic Design of TDOT Bridges in West Tennessee. **Alidadi, N.**, S. Pezeshk, and M. Davatgari Tafreshi (University of Memphis)
- S5-2** Near-Surface Site Characterization in West Texas Using Smart Solo Arrays and Passive Seismic Techniques. **Arthur, L.**<sup>1</sup>, H. Deshon<sup>2</sup>, J. Tung<sup>3</sup> (1: Texas A&M University; 2: Southern Methodist University; 3: Texas Tech University)
- S5-3** Spatial-Temporal Evolution of Microseismic Source Properties During Geothermal Stimulation: Insights from Utah FORGE. **Asirifi, R.** and X. Chen (Texas A&M University)
- S5-4** Benchmarking Machine Learning Pickers and Pre-trained Models for Earthquake Monitoring in Southeastern New Mexico. **Aziz Zanjani, A.**, U. Basu, and A. Record (New Mexico Tech)
- S5-5** Determine Crustal Q Structure from Ambient Noise Data. **Bera, A.** and L. Zhu (Saint Louis University)
- S5-6** Assessment of Availability and Accessibility of Hazard Warnings in Cascadia to Improve Equity in Disaster Risk Reduction. **Coker, S.**, M. R. Brudzinski (Miami University)
- S5-7** Characterizing Decadal Seismicity Patterns of Fault Patches in the Mexico Subduction Zone via Template Matching. **Khalkhali, M.**, M. R. Brudzinski, W. Ventura-Valentin (Miami University)
- S5-8** Radial Anisotropy beneath the North American Midcontinent. **Li, H.**<sup>1</sup>, X. Yang<sup>1</sup>, B. Herr<sup>2</sup>, B. He<sup>1</sup>, L. Liu<sup>3</sup>, A. S. Goddard<sup>4</sup> (1: Purdue University; 2: Rice University; 3: Chinese Academy of Sciences; 4: Indiana University)

- S5-9** Seismic Monitoring and Dynamic Triggering around the Santa Ana Volcanic Complex in Western El Salvador. Martinez-Coto, A., Navin Thapa, and Thomas H. W. Goebel (CERI, University of Memphis)
- S5-10** Comparison of 2D, 2.5D and 3D Electric Resistivity model in detecting shallow sub surface faulting. Mitra, I.<sup>1</sup>, R.T. Cox<sup>1</sup>, M.H.Loke<sup>2</sup>, K. Karki<sup>1</sup>, S. Islam<sup>1</sup>, C.H. Cramer<sup>1</sup> (1: University of Memphis; 2: Geotomo Software)
- S5-11** Enhanced earthquake detection in Snyder, Texas using LOC-FLOW with dense SmartSolo deployment and TexNet stations. Montazeri, S.<sup>1</sup>, X. Chen<sup>1</sup>, L. Arthur<sup>1</sup>, H. Deshon<sup>2</sup>, Jay Tung<sup>3</sup> (1: Texas A&M University; 2: Southern Methodist University; 3: Texas Tech University)
- S5-12** Referenced Empirical Ground-Motion Models for Arias Intensity, Cumulative Absolute Velocity, and Significant Durations for the Alborz Region of Northern Iran. Pakniat, S., S. Pezeshk, M. Davatgari-Tafreshi (University of Memphis)
- S5-13** Investigating Potential Relationships Between Rates of Seismicity, Strain Accumulation, and Slow Slip in the Oaxaca Region of Mexico. Szucs, E.<sup>1</sup>, M. R. Brudzinski<sup>1</sup>, S. Graham<sup>2</sup>, E. Cabral-Cano<sup>3</sup>, W. Ventura-Valentin<sup>4</sup>, M. Khalkhali<sup>1</sup> (1: Miami University; 2: The College of New Jersey; 3: Universidad Nacional Autnoma de Mxico; 4: Southern Indiana University)

### Session S6 (Oral): General. Session Chair: Heather DeShon

- 15:45–16:00 S6-1** Comparative analysis of background seismicity rate estimates and their uncertainties in tectonic and volcanic environments. Rinty, S., THW Goebel (University of Memphis)
- 16:00–16:15 S6-2** Joint Inversion of tau-p body wave and surface wave phase velocity dispersion to determine shallow Earth structure: Application to the OSIRIS-REx Capsule Return. Bazargan, S., C. Langston (CERI, University of Memphis)
- 16:15–16:30 S6-3** Comparison of Earthquake Wavefield Measurements from DAS and a Broadband Seismic Array in an Urban Setting. J. Sharma, Arrowsmith, S., H. DeShon, C. Hayward (Southern Methodist University)
- 16:30–16:45 S6-4** Characterizing earthquake source processes using nodal array. Chen, X., P. Ogwari, J. Walter (Texas A&M University)
- 16:45–17:00 S6-5** Seismic Catalog Development North of Puerto Rico and the Virgin Islands Using Machine Learning and Ocean Bottom Seismometers. Aziz Zanjani, A.<sup>1</sup> and H. DeShon<sup>2</sup> (1: New Mexico Tech; 2: Southern Methodist University)

### Session SB (Oral): Banquet Dinner. Session Chair: Linda Warren

- 18:30–19:15 SB-1** The Great Tornado of 1925. Wiegenstein, S. (Author)

## 2 Tuesday, October 28

**Session S7 (Oral): Earthquake Ground-Motion for the Central and Eastern United States, with a Focus on the Gulf and Atlantic Coastal Plains.** Session Chair: Shahram Pezeshk

**08:30–08:45 S7-1** A New Ground Motion Model Considering Sediment Thickness for the Coastal Plain Region of the USA. **Davatgari-Tafreshi, M.**<sup>1</sup>, M. Akhani<sup>2</sup>, and S. Pezeshk<sup>1</sup> (1: University of Memphis; 2: WSP in the US)

**08:45–09:00 S7-2** Lg Q Tomography for Crustal Attenuation and Site Amplification Across the Central and Eastern United States. **Cramer, C.**<sup>1</sup>, Anurhada Mahanama<sup>1</sup>, and W. Levendowski<sup>2</sup> (1: CERI, University of Memphis; 2: Tetra Tech, Inc.)

**09:00–09:15 S7-3** Constructing an Intensity Prediction Equation as a Step Toward Characterizing Site Amplification with DYFI Data. **Meyer, E.**<sup>1</sup>, L. G. Baise<sup>1</sup>, M. Roberts<sup>1</sup>, S. Nie<sup>1</sup>, and J. Kaklamanos<sup>2</sup> (1: Tufts University; 2: Merrimack College)

## Session S8 (Posters): 09:15–10:15 General

**S8-1** Use of Repeating Earthquakes to Discriminate Slow Earthquakes in the Central Pacific Subduction Zone of Costa Rica. **Campos, N.** and E. Chaves (OVSICORI-UNA)

**S8-2** Toward Characterizing Groundwater in the Jackson Purchase Region, Kentucky, with a Temporary Seismic Array. **Carpenter, S.**, F. Rodriguez Cardozo, E.G. Beck, A. Araji, J. Braunmiller, J.P. Schmidt, and E.W. Woolery (Kentucky Geological Survey, University of Kentucky)

**S8-3** Discriminating Volcanic and Tectonic Events in Western El Salvador based on Spectral Characteristics: Preliminary Insights on Site Effects. **Delgado-Andino, S.**, T. Goebel and D. Figueroa (CERI, University of Memphis)

**S8-4** Estimation of Relative Magnitudes and Spectral Characteristics of Acoustic Emission Events during Granular Shear. **Zambrano, E.**, T. H. Goebel (University of Memphis)

**S8-5** Long Term Monitoring of the Elgin-Lugoff, South Carolina Earthquake Swarm Using a Single Station Template Matching Method. **Jaume, S.**<sup>1</sup>, O. Adeboboye<sup>2</sup> and Z. Peng<sup>2</sup> (1: College of Charleston; 2: Georgia Tech)

**S8-6** Investigation of the Subsurface Structure of the Chestnut Hill Reservoir Earth Embankment Dam Using Ground Penetrating Radar (GPR). **Olawoyin, V.**, J. E. Ebel, E. Petschek (Boston College)

**S8-7** The 20 June 2025 Mw 4.9 Event in the Central Alborz, Iran: A Rare Tectonic Normal-Oblique Faulting Earthquake within a Complex Transpressional Regime. **Rodriguez-Cardozo, F.**<sup>1</sup>, J. Braunmiller<sup>1</sup>, C. Tape<sup>2</sup>, A. Ghods<sup>3</sup>, J. Hu<sup>4</sup>, S. Pham<sup>4</sup>, J. Thurin<sup>2</sup>, H. Tkali<sup>4</sup> (1: University of South Florida; 2: University of Alaska in Fairbanks; 3: Institute for Advanced Studies in Basic Sciences; 4: Australian National University)

**S8-8** Hydraulic Fracturing-Induced Seismicity Near the Cambridge Arch: Analysis of an Earthquake Swarm in Northern Noble County, Ohio, USA. **Fox, J.** (Ohio Department of Natural Resources, Division of Geological Survey)

**S8-9** Comparing Matched Filter and Machine Learning Detection of potentially Induced Seismicity near Snyder, TX. **Hlavac, J.**, X. Chen, S. Montazeri, L. Arthur, H. DeShon, and J. Tung (Texas A&M University)

- S8-10** Multifaceted Drivers and Distributed Fluid Injections Orchestrate Earthquake Swarms beneath the Eastern Himalayan Syntaxis. **Ma, J.**<sup>1</sup>, L. Meng<sup>2</sup>, M. Jiang<sup>1</sup>, H. Zhang<sup>3</sup>, G. Hou<sup>1</sup>, Y. He<sup>1</sup>, L. Li<sup>1</sup>, Z. Li<sup>1</sup>, M.-Y. Cai<sup>1</sup>, Y. Feng<sup>1</sup>, Y. Ai<sup>1</sup>, and L. Ding<sup>3</sup> (1: IGG, Chinese Academy of Sciences; 2: UCLA; 3: ITP, Chinese Academy of Sciences)
- S8-11** Investigating Human Induced Seismicity in the Eagle Ford Shale Play: Evidence for Hydraulic Fracturing Correlating with Increasing Magnitudes of Seismicity. **Mazzio, K.**<sup>1</sup>, M. Brudzinski<sup>1</sup>, A. Reedy<sup>2</sup>, J. Kirchenwitz<sup>1</sup> (1: Miami University; 2: Fort Valley State University)
- S8-12** Lessons Learned from Induced Earthquakes in the Southern Sichuan Basin, China. **Yang, H.**<sup>1</sup>, Jinping Zi<sup>2</sup>, Jiewen Zhang<sup>1</sup>, Aqeel Abbas<sup>2</sup>, and Yuyun Yang<sup>3</sup> (1: The Chinese University of Hong Kong; 2: SZRI, The Chinese University of Hong Kong; 3: Lingnan University)
- S8-13** Identification of Tornado Seismic Signals (TSS) in the Central United States. **Thompson, S.**<sup>1</sup>, N.S. Carpenter<sup>1</sup>, Y. Suni<sup>2</sup>, Z. Wang<sup>3</sup>, E.W. Woolery<sup>3</sup> (1: University of Kentucky; 2: Baylor University; 3: Kentucky Geological Survey)
- S8-14** Tracing Tennessee Tremors, the Construction of a Historic Seismicity Map for the State of Tennessee. **Moran, N.**<sup>1</sup>, William Jackson<sup>2</sup>, Valerie Harrison<sup>2</sup>, Maxwell O'Hearn<sup>3</sup> (1: CERI, University of Memphis; 2: Tennessee Geological Survey; 3: University of Memphis)

**Session S9 (Oral): Induced and Exotic Seismicities. Session Chair: Michael Brudzinski**

- 10:15–10:30 S9-1** Interplay of Wastewater Injection and Hydraulic Fracturing in Induced Seismicity near Kingfisher, Oklahoma (20192024). **Ogwari, P.**, J. Walter, H. Xiao, I. Woelfel, A. Thiel, N. Gregg, B. Mace (Oklahoma Geological Survey)
- 10:30–10:45 S9-2** An Advanced Detection and Relocation Workflow for Characterizing Seismicity Associated with Hydraulic Fracturing in the Eagle Ford Basin, Texas. **Kirchenwitz, J.**, M. R. Brudzinski, K. Mazzio, M. Khalkhali (Miami University)
- 10:45–11:00 S9-3** Surface/near-surface seismic events near Atlanta, Georgia: natural or anthropogenic? **Z. Peng, Ding, C.**, M. Snook, and X. Si (Georgia Tech)
- 11:00–11:15 S9-4** Seismic Analyses of Quarry Blasts in NW Miami, Florida, 2019-2025. **McNutt, S.** (University of South Florida)
- 11:15–11:30 S9-5** Source Mechanism Analysis of Iceshelf Microseismicity Using Full Moment Tensor Inversion. **Aziz Zanjani, F.**, D. A. Wiens, M. E. Wysession (Washington University in St. Louis)
- 11:30–11:45 S9-6** Machine learning for effective microseismicity monitoring: dataset, benchmarks, and adaptable models for carbon sequestration in Oklahoma. **Xiao, H.**, J. Walter (University of Oklahoma)

**Session SM (Oral): Macelwane Lectures. Session Chair: Lupei Zhu**

- 14:15–15:00 SM-1** When the Earth Quakes: Father James B. Macelwane and the Institute of Technology. **Waide, J.** (Archivist Emeritus, Saint Louis University)
- 15:00–15:45 SM-2** A Century of Seismic Instrumentation. **Herrmann, R.** (Professor Emeritus, Saint Louis University)
- 15:45–16:30 SM-3** The Role of Seismologists in National Defense. **Woods, M.** (Geophysicist, Air Force Technical Applications Center)

### 3 Meeting Abstracts

(In the alphabetic order of the **presenter's** last name with underline indicating student)

**S5-1** Site-Specific Seismic Design of TDOT Bridges in West Tennessee. **Alidadi, N.**, S. Pezeshk, and M. Davatgari Tafreshi (University of Memphis)

Site-specific analyses may be required for bridges located in unique conditions, such as regions prone to long-duration earthquakes, near-fault zones, sites with critical infrastructure, or areas with specific soil characteristics. These analyses may decrease spectral acceleration demands compared to the uniform seismic hazard values provided by standard procedures, such as the AASHTO LRFD Bridge Design Specifications and the AASHTO Guide Specifications for LRFD Seismic Bridge Design. As a result, they can lead to more economical seismic designs and reduced construction costs for bridges. This study conducts site-specific ground motion response analysis (SSGMRA) for 32 bridge sites across Western Tennessee. Field tests include Multi-channel Analysis of Surface Waves (MASW) and Refraction Microtremor (ReMi) performed at 12 sites, while existing data from the Tennessee Department of Transportation (TDOT) supported the remaining locations. Site selection was based on the TDOT bridge locations, with a maximum spacing of 20 km between sites and the availability of borehole data. Dispersion curves from MASW and ReMi surveys were integrated and inverted to generate detailed shear-wave velocity ( $V_s$ ) profiles for each site. Site-specific analysis began with a Probabilistic Seismic Hazard Analysis (PSHA), followed by the development of the Uniform Hazard Response Spectrum (UHRS) at the B/C boundary. Deaggregation of the hazard results was performed to identify the mean and modal earthquake magnitudes and distances. Based on these parameters, ground motions were selected, scaled, and spectrally matched. To represent site conditions, shear-wave velocity profiles were randomized, and nonlinear soil properties

were assigned. Finally, site response analysis was conducted to derive surface response spectra for each site.

**S6-3** Comparison of Earthquake Wavefield Measurements from DAS and a Broadband Seismic Array in an Urban Setting. J. Sharma, **Arrowsmith, S.**, H. DeShon, C. Hayward (Southern Methodist University)

We compare earthquake wavefield measurements from a ~95 km urban dark fiber Distributed Acoustic Sensing (DAS) array and a co-located 16 km aperture broadband seismic array in Dallas, Texas. Using data from a regional M5.2 earthquake, we assess the ability of DAS to recover ground motion amplitudes and wavefield direction-of-arrival (DOA). Surface wave amplitude ratios between broadband and DAS range from 0.34 to 30.5, revealing significantly more heterogeneous DAS coupling than previously reported. While broadband sensors provide consistent amplitude and high-quality DOA estimates across all phases (P, S, and Rayleigh), DAS data show large amplitude variability unrelated to fiber orientation, suggesting coupling and emplacement differences as dominant factors. Signal coherence in DAS is also highly variable, with some segments showing stronger correlations during pre-event noise than during the earthquake signal. Nonetheless, by applying hierarchical clustering to inter-channel cross-correlations, we identify a 36-channel DAS subgroup suitable for array processing and obtain a robust DOA estimate for the Rayleigh wave within 2 of that derived from the broadband array. These results highlight both the promise and limitations of using urban dark fiber DAS for earthquake monitoring, and underscore the need for careful characterization of fiber coupling and geometry to enable reliable wavefield reconstruction.

**S5-2** Near-Surface Site Characterization in West Texas Using Smart Solo Arrays and Passive Seismic Techniques. **Arthur, L.**<sup>1</sup>, H. Deshon<sup>2</sup>, J.

Tung<sup>3</sup> (1: Texas A&M University; 2: Southern Methodist University; 3: Texas Tech University)

Accurate near-surface site characterization is essential for understanding local seismic response, especially in sediment-dominated regions like West Texas. To address this need, we conducted a four-month deployment of 20 Smart-Solo IGUs across the Snyder and Midland areas. The goal of this study is to characterize lateral and vertical variations in near-surface shear-wave velocity structure using passive seismic data. To evaluate the ambient noise environment, we computed Power Spectral Density (PSD) estimates for each station using continuous waveform data recorded by the Smart-Solo units. Data were segmented into day- and night-time windows in local time, and PSDs were calculated using Welch's method with appropriate window lengths and overlap to ensure stable spectral estimates. Instrument response was removed to obtain true ground velocity spectra. These PSDs reveal consistent diurnal variations in noise levels, with nighttime data offering lower contamination in the 0.510 Hz band, frequencies most sensitive to near-surface conditions. Building on this, we will apply the Horizontal-to-Vertical Spectral Ratio (HVSR) technique to extract predominant resonance frequencies at each node location. HVSR peaks will guide inversion for 1D shear-wave velocity ( $V_s$ ) profiles, providing in-depth knowledge into sediment thickness and subsurface impedance contrasts. The combination of PSD-informed data selection and HVSR-based inversion offers a cost-effective approach to mapping near-surface variability across geologically diverse sites. This study demonstrates the potential of temporary nodal arrays and passive seismic methods for regional-scale site response investigations and contributes to improving seismic hazard assessments in stable continental regions.

**S5-3** Spatial-Temporal Evolution of Microseismic Source Properties During Geothermal Stimulation: Insights from Utah FORGE.  
**Asirifi, R.** and X. Chen (Texas A&M University)

We investigate microseismic source properties during EGS stimulation at the Utah Frontier Observatory for Research in Geothermal Energy (FORGE), an experimental Enhanced Geothermal System (EGS) site. Persistent spatial variation in earthquake source parameters across fault zones reflects underlying heterogeneity that governs rupture processes. For fluid-driven seismicity, multiple investigations have documented spatial and temporal evolution of stress drop values that are consistent with reduced fault strength resulting from increased pore pressure conditions. Early-stage fluid-driven earthquake swarms, whether from wastewater injection or natural fluid processes, commonly exhibit characteristically low stress drops, with similar patterns observed near injection wells in geothermal fields during initial stimulation phases. However, accurate source parameter estimation is often complicated by attenuation corrections and methodological dependencies. To overcome these challenges, we analyze FORGE stimulation seismicity using waveform cross-correlation to identify event clusters that share similar waveforms and apply the empirical Greens function (EGF) method to resolve source time functions and spectral ratios. The EGF methodology offers distinct advantages for resolving detailed source processes and source complexity by effectively removing path and site effects. This approach enables high-resolution characterization of stress drops, source complexity, and fault or asperity behavior under fluid injection. Our results highlight persistent fault heterogeneity and pore-pressuredriven strength reduction in governing source processes, with implications for understanding induced seismicity and managing seismic hazards in enhanced geothermal systems.

**S5-4** Benchmarking Machine Learning Pickers and Pre-trained Models for Earthquake Monitoring in Southeastern New Mexico. **Aziz Zanjani, A.**, U. Basu, and A. Record (New Mexico Tech)

Increasing seismicity in regions with little to no historical earthquake activity has become a growing concern associated with energy develop-

ment across parts of the United States. In southeastern New Mexico, deep fluid injection has elevated pore pressures by more than 2.4 MPa near some basement faults (Smye et al., 2024), coinciding with the recent occurrence of earthquakes exceeding magnitude 3.5. To better understand the spatial and temporal relationships between injection-driven pore pressure changes and fault stability, a complete and high-resolution earthquake catalog is essential. To address this need, the New Mexico Institute of Mining and Technology is expanding its seismic monitoring network (SC) in the region. Complementing these efforts, this study aims to improve catalog completeness and resolution since 2020 through the application of machine learning (ML) detection methods and event relocation techniques. We evaluate the performance of different pre-trained models and ML pickers on seismic data from the SC, TX, and GM networks by benchmarking them against a reviewed catalog. The ultimate goal is to develop and optimize an automated workflow for seismic cataloging, enhancing the ability to monitor induced seismicity down to smaller magnitudes and support rapid operational response.

**S6-5** Seismic Catalog Development North of Puerto Rico and the Virgin Islands Using Machine Learning and Ocean Bottom Seismometers. **Aziz Zanjani, A.<sup>1</sup>** and H. DeShon<sup>2</sup> (1: New Mexico Tech; 2: Southern Methodist University)

The Puerto Rico Trench, north of Puerto Rico and the Virgin Islands, is defined by highly oblique subduction and significant offshore seismicity. However, limited azimuthal coverage from the land-based Puerto Rico Seismic Network (PRSN) has led to a sparse and low-resolution earthquake catalog in this region. This study integrates data from six USGS-operated ocean bottom seismometers (OBS), deployed offshore from mid-2015 to mid-2016, with land-based stations of PRSN to build a high-resolution seismic catalog. Using the SeisBench platform, we evaluate multiple pre-trained machine learning models, applying different models to OBS and land-based waveforms. We em-

ploy PhaseNet for phase picking and GaMMA for event association. The resulting catalog with aggregated ML picks includes 7,209 events, with 56,719 P-wave and 30,121 S-wave picks of which 11,924 P and 7,231 S picks are unique to the OBS network greatly enhancing offshore event coverage. We further refine event locations using waveform cross-correlation and relocation techniques. This improved offshore catalog enables better detection of seismic swarms and provides new insights into strain accumulation along the trench, supporting more accurate regional seismic hazard assessments.

**S9-5** Source Mechanism Analysis of Iceshelf Microseismicity Using Full Moment Tensor Inversion. **Aziz Zanjani, F.**, D. A. Wiens, M. E. Wysession (Washington University in St. Louis)

We present a moment tensor inversion methodology applied to microseismic icequake events recorded by broadband seismographs to characterize source mechanisms in complex stratified media. We perform full-moment-tensor inversions using the Computer Programs in Seismology (CPS) package (Herrmann., 2013), incorporating Green's function computations for a layered medium composed of surface firn, ice, water, sediments, and basement. The velocity structure is based on dispersion curve analysis (Diez et al., 2016) and Bedmap3 (Pritchard et al., 2024). Analysis reveals prominent extensional Lamb-wave arrivals at 2.8-3.2 km/s that are successfully modeled by Green's functions. To address inherent uncertainties in catalog event locations and origin times, we conduct inversions on a grid surrounding each source location and select optimal solutions for centroid and timing parameters. Results show all centroid depths within 40 meters of the surface, with moment magnitudes (Mw) ranging from 0.4-0.7. Moment tensor solutions reveal tensile crack opening and normal faulting mechanisms, indicating extensional stress regimes. The methodology successfully differentiates between double-couple, compensated linear vector dipole (CLVD), and isotropic source components, advancing moment tensor techniques for small-

magnitude events in layered environments with applications to ice-quakes, induced seismicity, volcanic processes, etc.

**S2-1** A Seismic Array over the SW Arm of the NMSZ. Bazargan, S.<sup>1</sup>, S. Horton<sup>1</sup>, C. Langston<sup>1</sup>, S. Ausbrooks<sup>2</sup> (1: CERI, University of Memphis; 2: Office of the State Geologist of Arkansas)

CERI deployed an ~800m aperture array consisting of 19 5-Hz Magsies-Fairfield seismic nodals in a cross pattern near Blytheville, AR on June 18, 2025. The array is several km west of the SW segment of the NMSZ. Three earthquakes (m2.0,2.6,3.1) located by the CNMSN within 9km were well recorded by the array. Back-azimuths calculated from broadband frequency-wavenumber (BBFK) analysis of vertical components agree with the CNMSN locations; slowness values are consistent with body-waves from reported depths, and S-P times are consistent with reported hypocentral distances. Also, four smaller earthquakes were observed in the recorded data that were not located by the CNMSN. Their azimuth and slowness from BBFK are consistent with location along the same part of the SW segment of the NMSZ. Continuous Wavelet Transform (CWT) analysis of these smaller earthquakes increased waveform signal-to-noise improving P-wave and S-wave arrival time picks. A primary goal of the array is to detect and locate earthquakes below the detection threshold (~m2.0) of the CNMSN. To test earthquake detection capability using BBFK, we ran BBFK for 1-minute windows for 30 consecutive minutes centered on the origin time of the m2.6 earthquake. Preceding the earthquake, we found consistent high slowness ~0.5s/km and azimuth ~121 in all windows consistent with ambient noise (e.g. surface waves with high slowness). In the window containing the earthquake, the azimuth shifted to 180 and slowness to 0.112s/km consistent with body waves from a 13.4km deep earthquake located south of the array. Following the earthquake, ambient noise again dominated the BBFK windows. This suggests we can automate the BBFK procedure to analyze 1-minute

windows of continuous data with a detection-test based on slowness below a threshold value (e.g. 0.22s/km). We can then apply CWT for positive test-windows to improve signal to noise and pick S-P times to constrain the distance.

**S6-2** Joint Inversion of tau-p body wave and surface wave phase velocity dispersion to determine shallow Earth structure: Application to the OSIRIS-REx Capsule Return. Bazargan, S., C. Langston (CERI, University of Memphis)

We implemented joint inversion of body and surface wave data to obtain velocity structure for two sites in Eureka County, Nevada, where we recorded seismic waves generated by the sonic boom of NASA's OSIRIS-REx capsule reentry in September 2023. We deployed two 96-m-long refraction surveys which aimed to investigate the velocity structure of the near surface and examine the acoustic-to-seismic coupling. The resulting body wave velocity model, derived from P wave travel times, is a 5-layer model ranging from 0.28 km/s at the surface to 1.2 km/s at 32 m depth. The inverted surface wave velocity model, derived from fitting the phase velocity dispersion curve, spans from 0.2 km/s at the surface to 0.96 km/s at a depth of 35 m using a model parameterized by velocity nodes with linear velocity gradients in between. We use Occams inversion in an effort to find both the relationship between P and S wave velocity structure and a consistent parameterized velocity model in terms of velocity nodes. This method leverages the combined sensitivities of both data sets. In this approach, we considered the intercept time as a function of P wave velocity and ray parameter in combination with surface wave phase velocity dispersion. We then linearized the inversion by expanding intercept time in a first order Taylor's series and solved this problem iteratively with singular value decomposition.

**S5-5** Determine Crustal Q Structure from Ambient Noise Data. Bera, A. and L. Zhu (Saint Louis University)

The amplitude of seismic wave is essential for

estimating intrinsic attenuation measured by the quality factor ( $Q$ ), which provides valuable information about the Earth's structure. Empirical Greens functions from ambient noise cross-correlation are used to estimate  $Q$  in an area with very few or no earthquakes. However, many cross-correlation methods fail to preserve the true amplitudes of Greens functions due to spectra whitening or one-bit normalization of noise. Magrini & Boschi (2021) proposed a frequency-domain cross-correlation normalized by the average auto-correlation of noises of all available receivers which preserves the amplitude decay information. They developed a non-linear inversion to estimate the amplitude decay coefficient  $\alpha(f)$  in regional and continental scales. Here, we first verified their cross-correlation method using synthetic data in an area of 700600 km<sup>2</sup>. We calculated surface-source Greens functions using the 1-D central US velocity model. Synthetic noise data are generated by summing all contributions from randomly distributed surface sources. We then divided the noise recordings into segments of 1 hr long and perform the normalized cross-correlation between segments of each pair of stations and stacked the results. We found that although the normalized ambient noise cross-correlation spectrum matches the model prediction in shape, a distance and frequency independent multiplier is needed to match the amplitudes of spectra. We developed a linear inversion to determine the multiplier and  $\alpha(f)$ . We also inverted the obtained  $\alpha(f)$  for 1-D crustal  $Q$  structure. Our synthetic tests show that  $\alpha(f)$  has practically zero sensitivity to the P-wave attenuation ( $Q_p$ ) due to that the data are dominated by the Rayleigh surface waves, but we were able to determine the S-wave attenuation ( $Q_s$ ).

**S8-1** Use of Repeating Earthquakes to Discriminate Slow Earthquakes in the Central Pacific Subduction Zone of Costa Rica. Campos, N. and E. Chaves (OVSICORI-UNA)

The complexity and dynamics of subduction zones exhibit a mix of fast (seismic) and slow (aseismic) slip, whose physical interaction

strongly influences fault system behavior and can promote the nucleation of potentially catastrophic events. Therefore, understanding how seismic and aseismic processes interact is crucial to improve earthquake hazard assessment. Repeating earthquakes (RE), events with highly similar waveforms and magnitudes that rupture the same fault patch at different times, provide a unique opportunity to advance our understanding of this complex relationship. Using the local seismic network and modern template-matching techniques, we studied 20 RE families, with a total of 430 events ranging from 2010 to May 2025, located in the Central Costa Rica Subduction Zone, one of the most seismically active and heterogeneous regions in the country due to the subduction of seamounts and the presence of slow slip events (SSEs) every 22 months or less. We show how the spatiotemporal distribution of RE correlates with the occurrence of large earthquakes ( $M > 6.0$ ) and well-characterized SSE episodes. Additionally, the emergence of localized, uncatalogued SSEs with magnitudes below the detection threshold of GNSS but observed at the two closest stations is accompanied by tremors and the continued rupture of an abundant RE family including hundreds of events. The slip rate, calculated from RE assuming constant stress drop, agrees with the previously measured plate convergence rate. Our results suggest that, along with tectonic tremor, RE represents the seismic manifestation of SSEs and could be used as markers to indicate their occurrence, duration, and spatial distribution, especially in areas where GNSS networks are non-existent, lack resolution, or when their magnitude falls below the minimum required for standard identification and localization techniques.

**S3-4** Toward Defining the Northern Boundary of the Eastern Tennessee Seismic Zone. N. Carpenter, S., C. A. Powell, W. Levandowski, J. B. Hickman, J. P. Schmidt, Z. Peng, M. C. Chapman (Kentucky Geological Survey, University of Kentucky)

The recent 2018 M4.4 Decatur and 2025 M4.1 Greenback, Tennessee, earthquakes serve

as reminders that the Eastern Tennessee Seismic Zone (ETSZ) can produce consequential events. Though its boundaries are uncertain, the ETSZ appears to occupy parts of at least six states, and its >300-km length implies that it can produce destructive earthquakes exceeding M7. Most ETSZ seismicity occurs in the zones central part, adjacent to and southeast of the New York-Alabama magnetic lineament (NY-AL). However, larger instrumentally recorded earthquakes with magnitudes  $\geq 4.0$  have occurred in nearly equal numbers on both sides of the lineament and throughout the zone, from northern Alabama to southeast Kentucky. Seismicity in Tennessee north of the central ETSZ coincides with a negative P-wave velocity anomaly at seismogenic depths. This band of seismic activity continues into southeastern Kentucky, but its association with the negative velocity anomaly is presently unknown. Numerous focal mechanisms in the more active parts of the ETSZ reveal an oblique-tensile stress condition. The only focal mechanism determined in southeast Kentucky is consistent with this stress state, but additional focal mechanisms are needed to delineate the stress regime. Very low seismicity rates appear to be associated with mapped tectonic structures in eastern Kentucky, suggesting possible zone boundaries. Seismic activity is nearly absent in the east-northeast-trending Rome Trough graben and in a large, positive isostatic gravity anomaly associated with mafic rift fill northwest of the seismicity band. Also, earthquakes are very rare southeast of the NY-AL in the north of Tennessee. These observations suggest that a complex set of crustal and possibly lithospheric-scale features may define the boundaries of the northern ETSZ. Enhanced seismicity and focal mechanism catalogs are needed to distinguish confidently between crust with and without ETSZ-type faulting and stress.

**S8-2** Toward Characterizing Groundwater in the Jackson Purchase Region, Kentucky, with a Temporary Seismic Array. **Carpenter, S.**, F. Rodriguez Cardozo, E.G. Beck, A. Araji, J. Braunmiller, J.P. Schmidt, and E.W. Woolery (Kentucky Geological Survey, University of Ken-

tucky)

Velocity variations ( $\Delta v/v$ ) determined from subtle changes in the codas of empirical Greens Functions of ambient seismic noise can be associated with near-surface property changes and used to infer groundwater level change. In this study, we are applying this methodology to quantify groundwater level fluctuations in the aquifers of the Kentucky part of the Mississippi Embayment, the Jackson Purchase Region (JPR), which support the regions water needs for agriculture, industry, and public water supply. Broadband seismic coverage is sparse in the JPR, and we are undertaking a multiyear investigation of a  $\sim 2,000$  km $^2$  area using a temporary seismic array. Based on previous studies and preliminary work in the larger Upper Mississippi Embayment, the necessary resolution requires seismometer spacing of  $\sim 10$  km or less and ambient noise recordings at frequencies  $\leq 0.2$  Hz. These requirements can be satisfied cost-effectively by deploying a dense array of broadband seismometers that reliably record weak, low-frequency seismic waves. Here, we present an overview of available groundwater and hydrostratigraphic data in the JPR, results from instrument evaluations, and preliminary empirical Greens Functions.

**S6-4** Characterizing earthquake source processes using nodal array. **Chen, X.**, P. Ogwari, J. Walther (Texas A&M University)

Earthquake source parameter characterization is often limited by data coverage and frequency bandwidth. For the same earthquake, different data processing strategies and instruments can lead to different results. Using southern California dataset, Chen et al., (2025) carefully compared the source characterization using regional seismic networks and DAS array. In Oklahoma, several dense nodal arrays are deployed in active fault zones to complement regional seismic networks. The colocation of temporary nodal array and long-term regional stations provide an opportunity to further probe source characterization. The Quinton sequence in south-

ern Oklahoma features diverse spectral contents with clusters enriched in low-frequency energy. Applying empirical Greens function analysis to the limited regional seismic stations (< 5), we find that a low frequency cluster is characterized by extended source duration and low stress drop, suggesting possible fluid-driven aseismic process. A temporary nodal array was deployed for 30 days before a M3 earthquake and recorded abundant seismicity. Three events have corner frequency estimates from both regional network and nodal array. Although the overall agreement is good, one event with higher corner frequency from nodal array was underestimated by the regional seismic network, likely due to the bandwidth limit. We will further calculate the stress drop and source time functions for additional events detected by the nodal array from machine learning and matched filter detection methods and compare with the general features with regional seismic network. The high sampling rate (500 Hz) and dense spatial coverage of the nodal array provide better resolution of small earthquakes, which can lead to better understanding of fluid-faulting interactions.

**S5-6** Assessment of Availability and Accessibility of Hazard Warnings in Cascadia to Improve Equity in Disaster Risk Reduction. Coker, S., M. R. Brudzinski (Miami University)

Effective multi-hazard early warning systems (MHEWS) are critical for achieving the United Nations' Sendai Framework target of increasing access to disaster risk information by 2030. This study presents an analysis of Oregon's OR-Alert system, examining 28,512 alerts and 9.6 million associated messages delivered over a nine-month period across 28 counties. We analyzed alert distribution patterns, communication methods, geographic coverage, and temporal variations to assess system applicability for integration of earthquake early warning (EEW) integration. Our results indicate that while OR-Alert demonstrates robust capacity potentially reaching over 2 million reported recipients, significant challenges remain. Push notification adoption remains very low at 2%, posing substantial barriers for time-

sensitive earthquake warnings. Geographic analysis reveals marked disparities in system enrollment, with some counties having high participation while some populous regions show less than 10% participation. Natural hazards comprise 70% of public alerts, delivered primarily through SMS (52%), with distinct seasonal patterns corresponding to regional hazard profiles. These findings highlight the need for targeted interventions to enhance push notification adoption, address coverage disparities, and optimize the system for rapid-onset hazard communication, particularly as the Cascadia region seeks to improve its EEW capabilities.

**S1-4** Gravity Models Suggest Fluid Processes Associated with Mississippi Embayment Conductive and Low Seismic Velocity Anomalies in the Crust and Mantle. **Cramer, C.** (CERI, University of Memphis)

Previous magnetotelluric (MT) and seismic velocity studies have identified conductive anomalies near embayment crustal faults and low velocity anomalies in the upper mantle. Embayment Cenozoic and Cretaceous sediments are known from previous geophysical and geological studies to be conductive, low density, and low velocity due to their fluvial depositional environment. 3D geology based seismic hazard studies of the embayment have defined the areal thickness and density of embayment sediments so their gravitational effects can be more accurately modeled. Gravity and magnetic studies have identified a lower crustal rift pillow beneath the Mississippi Valley Graben. We use this geophysical and geological information to model 2D gravity profiles from available regional complete Bouguer gravity data along four shallow MT profiles across the Axial Fault of the New Madrid seismic zone and the east bounding faults of the Mississippi Valley Graben. Additionally, we model a gravity profile along Geng et al.s (2020) profile C-C which reveals mantle seismic low velocity anomalies beneath the embayment. Our modeling suggests that low density is associated with the observed MT conductive anomalies near faults and that fluid or hydrous-

altered mineralogy is associated with the mantle velocity anomalies of Geng et al. (2020). Thus, gravity observations are consistent with fluids and their products being associated with these anomalies and compatible with previous suggestions of fluid processes being involved in the tectonic processes beneath the embayment.

**S2-2** Resistivity Structure of the Alabama-Oklahoma Lineament and the Mississippi Embayment. K. Sarker and **Cramer, C.** (CERI, University of Memphis)

The Alabama-Oklahoma Lineament (AOL) is a major structural boundary between the Southern US and Gulf Coast and cuts off the southern end of the Mississippi Embayment (ME). This study uses magnetotelluric data from the USArrayMT regional dataset to investigate the resistivity structure along and around the AOL and the ME and their role in the seismicity of the region. 2D inversions reveal a steeply dipping conductive anomaly ( $\sim$ 50-100 Ohm-m) separating high-resistivity blocks ( $\sim$ 500-1000 Ohm-m) that align with the AOL. The conductive features separate high heat-flow regions to the southwest of the lineament from low heat-flow regions to the northeast of the lineament. The electrically conductive nature of the AOL may suggest that the AOL represents a tectonic weak zone influencing crustal deformation and regional seismicity. The lithosphere below the ME has normal lithospheric resistivity of 500 to 1000 Ohm-m down to at least 100-150 km. This suggests a stronger crust capable of sustaining large M7 earthquakes such as those of the New Madrid seismic zone. However, near the western edge of the ME and north of the AOL there is a region of low lithospheric resistivity of about 10 Ohm-m beneath the Enola region of Arkansas. This conductive feature seems associated with a low seismic velocity lithospheric structure previously identified at a depth of about 100 km and deeper in that region. If due to the presence of fluid, it might explain the swarm character of the seismicity in that region.

**S7-2** Lg Q Tomography for Crustal Attenu-

ation and Site Amplification Across the Central and Eastern United States. **Cramer, C.**<sup>1</sup>, Anurhada Mahanama<sup>1</sup>, and W. Levendowski<sup>2</sup> (1: CERI, University of Memphis; 2: Tetra Tech, Inc.)

We present a new high-resolution model of crustal Lg-wave attenuation and site amplification across the Central and Eastern United States (CEUS), derived from joint tomographic inversions of vertical and horizontal seismic amplitudes. Using more than 75,000 broadband records from over 1,600 regional crustal earthquakes ( $M_w \geq 3.5$ , depth  $< 30$  km) recorded between 2007 and 2024 at more than 1,500 seismic stations, including data from the EarthScope Transportable Array (TA), N4, and other regional networks, we resolve frequency-dependent seismic quality factor (Q), site terms, and source amplitudes across five center frequencies from 0.7 to 11.3 Hz. Our results show significant lateral variations in attenuation, with  $Q_0$  values as low as  $\sim 200$  in sediment-rich, tectonically complex regions such as the Mississippi Embayment, Gulf and Atlantic Coastal Plains, and the Southern Oklahoma Aulacogen. In contrast, stable cratonic interiors such as the Permian Basin and Midcontinent exhibit high  $Q_0$  values (up to  $\sim 380$ ), reflecting cold, uniform basement crust. We also resolve frequency dependence of attenuation via the  $\eta$  parameter, which varies from  $\sim 0.7$  in high- $Q_0$  regions to  $> 1.0$  in areas with strong scattering. Site amplification terms show higher values in intracratonic basins and coastal plain sediments and lower values in regions with exposed or shallow bedrock. The horizontal-to-vertical site amplification ratio exhibits a polarity shift across the Coastal Plain boundary. This shift reflects the contrast in near-surface geology between flat-lying sediments and folded orogenic crust. Checkerboard and feature recovery tests demonstrate the models resolution capacity down to  $\sim 100$  km, and jackknife resampling confirms relative uncertainties below 2% across most of the domain. Compared to previous CEUS attenuation studies, our model benefits from denser station-event coverage and improved inversion methodology. These findings

provide critical input for refining seismic hazard assessments and updating ground motion prediction models for the next-generation U.S. National Seismic Hazard Model.

**S7-1** A New Ground Motion Model Considering Sediment Thickness for the Coastal Plain Region of the USA. **Davatgari-Tafreshi, M.**<sup>1</sup>, M. Akhani<sup>2</sup>, and S. Pezeshk<sup>1</sup> (1: University of Memphis; 2: WSP in the US)

In this study, we develop adjustment factors for the median NGA-East ground-motion models (GMMs), focusing on the Gulf Coast and Coastal Plain regions of the United States. In the region known as the Coastal Plain, we establish a set of adjustment factors based on sediment thickness and rupture distance. This study utilizes sediment thickness contour maps from Boyd et al. (2024) and a comprehensive dataset, which combines the NGA-East dataset (Goulet et al., 2014), the Chapman and Guo (2021) dataset, and the newly compiled and verified USGS dataset (Thompson et al., 2023). Residuals are calculated by subtracting the natural logarithm of the observed data from the predictions made by the median NGA-East GMMs. A mixed-effects regression partitions total residuals into between-event and within-event components. For stations within the Coastal Plain, adjustment factors are obtained by regressing within-event residuals using a functional form that includes sediment thickness and rupture distance. The results show that the proposed adjustment factors successfully reduce residual trends associated with site and path terms across most periods for stations within the Coastal Plain. These findings are relevant to seismic hazard and risk assessments for sites within the Coastal Plain.

**S4-2** Adventures in improving earthquake depth estimates, Texas. **DeShon, H.**, Y. Seldon, and J. Sharma (Southern Methodist University)

Machine learning (ML) phase detection and association has altered the landscape for the rapid creation of earthquake catalogs. Many

rapid deployments in urban areas use a mix of accelerometers and velocity sensors and have a complicated metadata history, creating scenarios the push the limits of available training datasets. The North Texas Earth Study (NTXES) in the Fort Worth Basin consists of rapidly deployed 1- and 3-component short-period, strong-motion, broadband, and nodal sensors in a large metropolitan area with changing configuration as seismicity evolved from 2008 to present. The NTXES catalog, with over 3000 earthquakes, was originally built using automated detection with manual review (Quinones et al., 2019). While the catalog provided fundamentally important data to understand physical mechanisms of induced seismicity in the basin, original efforts to constrain time variation in b-values, conduct nearest neighbor determinations, etc. were limited by incompleteness at both the high and low magnitude end of the catalog. Additionally, the earthquakes are quite shallow and low magnitude, further complicating depth resolution considering a strong near-surface velocity-depth trade-off curve. We present efforts to extend the catalog using PhaseNet (Zhu and Beroza, 2018) arrival time detections and show comparison with the manual catalog. We explore which training datasets best handle the mix of sensors present in the NTXES dataset. We will also show evidence of the velocity model-depth trade-off common in sedimentary basins and explore ways synthetic waveforms of converted phases point a way forward to better resolve depth, using examples from the Midland Basin.

**S8-3** Discriminating Volcanic and Tectonic Events in Western El Salvador based on Spectral Characteristics: Preliminary Insights on Site Effects. **Delgado-Andino, S.**, T. Goebel and D. Figueroa (CERI, University of Memphis)

The western part of El Salvador hosts the Santa Ana Volcanic Complex, one of the most active seismic and volcanic regions in the country. The seismicity in this region is driven by both volcanic processes and regional tectonics, from local faults to regional structures related

to the subduction zone. Discriminating between volcanic and non-volcanic earthquakes is crucial for improving hazard assessment and implementing early warning systems. For this purpose, the Generalized Inversion Technique (GIT) is implemented to identify potential source-spectral differences within depth-homogeneous clusters of earthquakes that share similar path effects. An important step for this spectral inversion is to determine the local site effects, due to its influence on the recorded seismic spectra. As a methodological contribution, the Horizontal to Vertical Spectral Ratio (HVSR) is employed to estimate the frequency-dependent site terms at each station that will help constrain the inversion results. The implementation of HVSR-based site response into the second inversion of the two steps GIT approach is expected to reduce trade-offs and improve the separation of source and path, thereby providing a more stable framework for spectral inversion. The data are drawn from 10 short period (Raspberry Shake) and 4 broadband stations maintained by the CERI, University of Memphis (University of Memphis), the University of El Salvador, and the Ministry of Environment and Natural Resources. The broader goal of this project is to establish a quantitative framework for discriminating volcanic from non-volcanic earthquakes in western El Salvador to improve monitoring capabilities, early warning, and hazard-mitigation strategies.

**S2-3** Statistical Properties of Early Aftershocks Following Moderate-size Earthquakes in the Central and Eastern United States. Ding, C.<sup>1</sup>, Z. Peng<sup>1</sup>, J. Zhuang<sup>2</sup>, and X. Si<sup>1</sup> (1: Georgia Tech; 2: Institute of Statistical Mathematics)

Early aftershocks provide valuable insights into the mainshock rupture properties and physical processes that control earthquake triggering following moderate-size to large earthquakes. However, detecting early aftershocks is challenging with overlapping aftershock waveforms in short time windows and strong coda waves from the mainshock. To address these limitations, various detection methods have been applied, including matched-filter and machine-

learning techniques. While these approaches have achieved some success in tectonically active regions, the detected aftershock rates likely reach the limitation of these techniques, likely due to the relatively high background seismicity rates in these regions. Because the background seismicity rates in the Central and Eastern United States (CEUS) are relatively lower than those in plate boundary regions, analyzing early aftershocks in the CEUS provides an excellent opportunity to resolve whether the seismicity remains flat or even increases (e.g., a physically meaningful  $c$  value in the modified Omoris law), before the Omoris law decay. In this study, we examine early aftershock behaviors following moderate-size ( $M > 4$ ) earthquakes in the CEUS region since 2000. Examples include the 2011 M5.7 Virginia, the 2020 M5.2 Sparta, and 2024 M4.8 New Jersey earthquakes. For each sequence, we replenish the early aftershock catalog by using the aftershocks detected at later times to examine what is the likely behavior when the Omoris law  $c$  value is very small. Manual inspection is also conducted within the first 12 days after each mainshock to recover potentially missed early aftershocks. Aftershock rates are then evaluated using both synthetic and observed catalogs. Our comparison reveals that several sequences lack clear early aftershock signals, suggesting a suppression of immediate aftershock activity, possibly due to the relatively low background rates in the regions. The findings from this research could significantly improve our understanding of aftershock behavior in intraplate regions and contribute to better seismic hazard assessments.

**S9-3** Surface/near-surface seismic events near Atlanta, Georgia: natural or anthropogenic? Z. Peng, Ding, C., M. Snook, and X. Si (Georgia Tech)

Regular crustal earthquakes occur at a few to a few tens of kilometers depth, also known as the seismogenic depth. However, extremely shallow earthquakes that are less than 2 km depth are sometimes found in the Southeastern U.S., mostly along the blue ridge and piedmont

regions. Here we report two additional cases of seismic events that occur on or within a few meters depth near Atlanta, Georgia. In the first case, a major rock exfoliation event was identified around noon on July 17, 2023 in a former Lithonia Gneiss quarry near Arabia Mountain, Georgia. Since April 2024, we have instrumented this region with multiple nodal seismic sensors sampling at 1000 /s. We recorded two small rock exfoliation events in Summer 2024, and one was captured in a video recording (<https://www.youtube.com/watch?v=MDvGrxGgKic>). These events have precursory signals, and are likely driven by thermal expansions due to surface heating. In the second case, homeowners at Social Circle, GA about one hour east of Atlanta reported repeated minor shaking and rumbling since August 14, 2025. The shaking repeated once every 6-10 minutes, and Georgia Tech team deployed multiple nodal stations on August 15, 2025. These events have source durations of 0.5 to 1 s, and the subevents appeared to propagate to the southeast with an apparent velocity of  $\sim$ 110 m/s. Their occurrence was first interpreted as a water-hammer effect due to choking of near-surface ground water flows. Subsequent ground penetrating radar (GPR) surveys and on-site excavations revealed that a faulty sewer pipe vibration as the primary cause of the repeated ground vibrations. These case studies provide additional evidence that surface and near-surface processes (either natural or man-made) are capable of generating seismic events, and properly recording them with dense on-site recordings (and ground-truth observations) can help to confirm their causes.

#### **S4-4 A Spatial Forecast of Some $Mw \geq 6.5$ Earthquakes in California and Nevada. Ebel, J. (Boston College)**

A previously published study (Ebel and Chambers, GJI, 2016) showed that the  $M \geq 4$  seismicity prior to several large California earthquakes occurred randomly along the future fault ruptures and at rates exceeding 0.5  $M \geq 4$  events per year. Building on this observation, this paper presents a prospective forecast of the loca-

tions of the next  $Mw \geq 6.5$  earthquakes in California and Nevada based on the locations and rates of occurrence of  $M \geq 4.0$  earthquakes during the past 30 years, called here preshocks. The time period of the forecast is arbitrarily set at 33 years. The forecast faults are the Anza section of the San Jacinto Fault, the Calaveras Fault, the creeping section of the San Andreas Fault, the Maacama Fault, the San Bernardino section of the San Jacinto Fault, and the southern San Andreas Fault, all strike-slip faults in California, and the normal-faulting Wassuk Range Fault in Nevada. The temporal history of preshocks for past  $M \geq 6.5$  earthquakes in California do not indicate when the future mainshock will occur. The probability of just one of the forecast events actually taking place during the forecast time period is less than 2%. Outside of California, preshock activity was observed before the 2016  $Mw 7.0$  Kumamoto, Japan earthquake, the 2023  $Mw 7.8$  Kahramanmaraş, Turkey earthquake, and the 2017  $Mw 6.5$  Juizhaigou, China earthquake, all strike-slip events, as well as the 2008  $Mw 7.9$  Wenchuan, China thrust earthquake, although the two mainshocks in China had preshock rates less than 0.5 events per year.

#### **S8-8 Hydraulic Fracturing-Induced Seismicity Near the Cambridge Arch: Analysis of an Earthquake Swarm in Northern Noble County, Ohio, USA. Fox, J. (Ohio Department of Natural Resources, Division of Geological Survey)**

The Ohio Geological Survey is studying a recent swarm of approximately 70 induced earthquakes in northern Noble County, Ohio, including three events of  $ML \geq 3.0$ , occurring along a northsouth-oriented fault subparallel to the Cambridge Cross-Strike Structural Discontinuity (CCSD). The seismic activity provides insights into reactivation of pre-existing structures in this geologically complex region within the Grenville Province and Appalachian Basin. The CCSD is a fault system that is part of an intra Grenville Province suture zone that comprises the Parkersburg-Lorain Syncline to the west and Cambridge Arch to the east. Overall, the CCSD is interpreted as a right-lateral

transpressional fault system with 4552 meters of vertical displacement, occurring along pre-existing zones of weakness defined by faults initiated during the Grenville Orogeny. Differential subsidence along faults of the CCSD form a hinge line where Silurian- and Devonian-age strata thicken eastward. They were subsequently uplifted by inversion forming the Cambridge Arch. Previous studies suggest repeated basement fault reactivation along the CCSD, indicating a complex deformation history. Analysis of the swarm reveals strong temporal correlation between hydraulic fracturing operations and seismic occurrences. Earthquake activity rapidly ceased following each pause in fracturing operations, dropping to background levels between stages. When injections resumed, seismic activity resumed rapidly, demonstrating a prompt fault response to pore pressure changes. This pattern repeated consistently across multiple operational cycles, indicating direct hydraulic communication between injection zones and the reactivated fault. These findings demonstrate that ancient structural features like the CCSD create zones of weakness that are particularly susceptible to induced seismicity. The immediate seismic response to operational changes emphasizes the critical importance of understanding pre-existing structural architecture when conducting hydraulic fracturing operations in tectonically complex regions of the eastern United States.

**S4-1** Why are foreshocks rare in nature?: A laboratory perspective on accelerating fault slip and earthquake nucleation. **Goebel, T.<sup>1</sup>, V. Schuster<sup>2</sup>, G. Kwiatek<sup>2</sup>, K. Pandey<sup>3</sup>, and G. Dresen<sup>2</sup>** (1: University of Memphis; 2: GFZ-Potsdam; 3: UES)

Dynamic slip in the laboratory is generally preceded by bursts of foreshocks which accompany a predominantly aseismic preparation process. Aseismic slip is also thought to govern earthquake nucleation in nature, yet, foreshocks are rare. This relative sparsity of foreshocks in nature may be due to differences in instrumentation, detectability of foreshocks, un-

derlying physics or due to the vastly different conditions at seismogenic depth. We examine the discrepancy of foreshocks in lab and nature, focusing on the impact of fluid pressure and fault roughness on duration and amplitude of premonitory signals before failure. We investigate seismic and aseismic processes at upper-crustal confining pressure on dry and fluid-saturated conditions with fluid pressures between 0.5 to 35 MPa. Our tests exhibit a complex coupling between incipient fracture geometry, evolving fault zone structure, damage and pore fluid pressure with the fault. At the micro-scale, higher fluid pressures shorten the duration of precursory seismic signals before slip and micro-seismicity is increasingly dominated by earthquake-like double-couple mechanisms. At the macro-scale, high fluid pressure reduce fault strength and stress drop but also promote more rapid slip-acceleration toward failure. These observations suggest that foreshocks are rare at pressures and stresses that govern earthquake nucleation. Gradual fault activation and extended foreshock activity is more likely observable before shallow earthquakes.

#### **S2-4** Fracture-Mediated Water Level Changes at a Groundwater Well in Virginia (2008-2025).

**Gribbins, J.<sup>1</sup>, J. Maynard<sup>2</sup>, S. Thompson<sup>1</sup>, R.J. Hung<sup>1</sup>, N.G. Randolph-Flagg<sup>1</sup>** (1: University of Kentucky; 2: Virginia Department of Environmental Quality)

Distant earthquakes can cause significant changes in groundwater levels, despite inducing only minimal elastic strain. Such changes have been observed for millennia across a wide range of tectonic, geologic, and hydrologic settings. A variety of conceptual and computational models have been proposed to understand these changes. We use 17 years of continuous data, collected at 5-minute intervals, from a 137-meter-deep limestone water well, intersected by a large fracture, in western Virginia to explore earthquake-induced changes. These changes were frequently exceeding 1 meter in response to earthquakes occurring thousands of kilometers away. By analyzing solid Earth tides, we track the evolution of

permeability, and, using conductivity data from 2017 and 2018, we examine concurrent changes in water chemistry. These observations provide insight into hydrologic processes occurring within fractures and faults, both at the surface and at seismogenic depths.

**S2-5** A New Joint Inversion Method for Constructing High-Resolution 1-D Crustal Seismic Velocity Structures. **Habib, M.** and L. Zhu (Saint Louis University)

We developed a new joint inversion method to use four different types of seismic data: surface wave dispersion, receiver function, Ps-delay times, and teleseismic waveforms to construct high-resolution 1-D crustal velocity models. We improved a previously developed joint inversion method of Liu and Zhu (2021) by replacing the PmP traveltimes with teleseismic S-waveforms because of the difficulty in measuring the PmP traveltimes and its lack of constraint on the Vp/Vs ratios of individual crustal layers. The new joint inversion method was tested with both noise-free and noise-added synthetic data. The results show improvements in the velocity models, especially the Vp/Vs ratios of different crustal layers. We also applied the method to data of a 300-km linear array across the Wabash Valley Seismic Zone in the Central United States. Using 108 teleseismic S-wave waveforms and previously obtained surface wave dispersions, receiver functions, and Ps-delay times data, we obtained 152 high-resolution 1-D models. We stitched the 1-D models to construct a 2-D image showing lateral variations in S-wave velocities, interface depths, and Vp/Vs ratios. The S-wave velocity increases gradually with depth but shows distinct anomalies. The upper crust has low seismic velocities with localized high-velocity anomalies, likely felsic to intermediate intrusions from past magmatism. In the middle to lower crust, a broad low-velocity anomaly suggests a weak zone with fluids. Just above the Moho, three pillow-shaped high-velocity anomalies appear, interpreted as solidified mafic intrusions from mantle-derived magmatism. A significant contrast in Vp/Vs ratios is observed between the upper and lower crust beneath the La Salle Deformation Belt. Higher Vp/Vs ratios (1.841.86) in the lower crust suggest fluid presence, while the overlying crust shows lower, stable ratios (1.801.85), consistent with felsic composition. These results demonstrate the effectiveness of teleseismic S-waveforms in constraining crustal velocity models, especially Vp/Vs ratios.

**S4-3** DYNAMIC TRIGGERING OF EARTHQUAKES IN COSTA RICA. **Hajaji, S.**<sup>1</sup> and E. Chaves<sup>2</sup> (1: Georgia Tech; 2: OVSICORI-UNA)

We document for the first time the dynamic triggering of earthquakes in Costa Rica due to teleseismic events. Dynamically-triggered failure is typically observed in volcanic or geothermal settings, characterized by the presence of fluid flow and/or high pore pressures weakening fault settings by reducing the normal effective stress, and has been found to be less common in continental or local faults and subduction zones. We use OVSICORI's broadband seismic stations in Costa Rica to look for teleseismic events from 2010 until February 2023. We recovered a total of 25 events, and two events were identified as prime examples of triggering during the arrival of surface waves: the 2018 Mw 7.5 North of Honduras earthquake and the 2023 Mw 7.8 Turkey earthquake. Both earthquakes share similarities, as they are strike slip and supershear events. These aspects are interesting, considering that most of the earthquakes in our catalog are dominated by the inverse mechanism. To evaluate whether a teleseismic event dynamically triggered or not and inspect the increase of the seismicity rate, we implemented three approaches: (1) visual inspection of seismograms in both time and frequency domains, (2) the  $\beta$  value statistic, and (3) probabilistic power spectral density (PPSD) analyses performed before and after the passage of teleseismic surface waves. This last technique is a novel method in dynamic triggering studies, providing a catalog independent approach that had not been previously applied like this for this purpose. Our results reveal that triggered seismicity occurred in three tectonically

distinct areas of Costa Rica: the northern volcanic region, the subduction zone interface off the southern Pacific coast, and shallow crustal faults in central Costa Rica. These findings highlight the presence of critically stressed faults in Costa Rica and demonstrate that dynamic triggering can be a valuable indicator of fault weakness.

**SM-2** A Century of Seismic Instrumentation.  
**Herrmann, R.** (Professor Emeritus, Saint Louis University)

**S2-6** Refining GPS Time Series Analysis for Strain Estimation in the New Madrid Seismic Zone. **Heydarizadeh Shali, H.**<sup>1</sup>, Robert Smalley<sup>1</sup>, Demian Gomez<sup>2</sup> (1: CERI, University of Memphis; 2: Ohio States University)

Continuous GPS (CGPS) stations provide precise measurements of baseline changes over time, enabling the study of subtle crustal deformation in low-strain regions such as the New Madrid Seismic Zone (NMSZ). However, detecting extremely slow deformation rates remains difficult due to atmospheric, hydrological, and instrumental noise, as well as stochastic variations in monument positions that may follow a random-walk (RW) process. In the presence of RW, it becomes nearly impossible to separate true linear motion from motion contaminated by RW components, making careful signal decomposition essential. Most GPS analyses employ standard trajectory modeling (TM) with annual and semi-annual terms, but this approach cannot fully capture the complexity of seasonal and hydrological signals. To address this, we apply an iterative framework that combines parametric TM with non-parametric Singular Spectrum Analysis (SSA), which better isolates cyclic signals and long-period or polynomial-like trend soften corresponding to genuine geophysical processes while improving characterization of residual noise. This approach reduces signal leakage, minimizes RW contamination, and more realistically accounts for noise accumulation in nearly two decades of CGPS velocity estimates. Finally, we evaluate the implications for strain estima-

tion using both grid-based approaches, which are sensitive to network geometry and station density, and baseline-based methods such as Delaunay triangulation, which directly estimate strain from interstation distances. The resulting strain rates are on the order of  $10^{-9}$ , consistent with previous peer studies. Together, these refinements yield a more reliable velocity field and provide a robust framework for quantifying tectonic strain in the NMSZ.

**S8-9** Comparing Matched Filter and Machine Learning Detection of potentially Induced Seismicity near Snyder, TX. **Hlavac, J.**, X. Chen, S. Montazeri, L. Arthur, H. DeShon, and J. Tung (Texas A&M University)

Subsurface fluid injection has driven a notable increase in seismic activity across the Permian Basin, including the Delaware Basin and the Midland Basin. The 2024 M5 Snyder earthquake sequence occurred at the eastern edge of the Midland Basin. This area has sparse wastewater disposal wells, but a large number of hydraulic fracturing wells. In late 2024, a nodal array was deployed near Snyder to capture detailed records of potentially induced seismicity, and understand the relationship with hydraulic fracturing and wastewater disposal activities. This study evaluates the performance of matched filter and machine learning detection approaches in identifying earthquake clusters recorded by the Snyder array. The matched filter technique uses 44 cataloged events as templates to detect small earthquakes using cross-correlation. The detection is followed by magnitude calibration with cataloged events using relative amplitude ratio. Preliminary analysis of five days detected 81–151 events (depending on the cutoff threshold), while only 7 cataloged events occurred during the same time period. The magnitude completeness reaches M-1 after magnitude calibration. These results will be compared against a complementary study using machine learning detections applied in the region during the same timeframe, allowing an assessment of each methods sensitivity, accuracy and efficiency. Analyzing the resulting clustered events and their

characteristics, we will investigate the underlying fault structures and their fluid injection response properties. This contributes to a more detailed understanding of the seismicity near Snyder, and offers insights into induced seismicity in the Midland Basin. Ultimately, this work will show the potential and limitations of different detection strategies in improving fault characterization of induced seismicity in hydrocarbon-producing regions like the Permian Basin.

**S8-5** Long Term Monitoring of the Elgin-Lugoff, South Carolina Earthquake Swarm Using a Single Station Template Matching Method.  
**Jaume, S.**<sup>1</sup>, O. Adeboye<sup>2</sup> and Z. Peng<sup>2</sup>  
(1: College of Charleston; 2: Georgia Tech)

A prolonged earthquake swarm occurred near the town of Elgin-Lugoff in South Carolina between 2021 and 2025, yet its physical mechanism remains known. Here, we apply a single station waveform template matching technique to detect small earthquakes in this sequence from 1630 UTC on December 21, 2021 through December 2024. Our analysis uses 90 template events, all located by the U. S. Geological Survey, to search for additional smaller magnitude earthquakes detected at the closest network station, CO.BARN. We calibrate this single station detection method using the results of a temporary dense nodal deployment in late fall of 2022 (Adeboye et al., 2025), finding a similarity level (0.5) that only matches earthquake events and not with other anthropogenic or natural events. We identify 467 additional earthquake events beyond those located by the regional South Carolina Seismic Network. Magnitudes were estimated using peak velocities at BARN calibrated to the magnitudes determined from the nodal deployment results. Earthquakes as large as M 1.85 are not detected by the regional network when they are in the coda of an even larger (M 3+) earthquakes. We also find other new events as large as M 1.55 not in the coda of larger events. Using the times and estimated magnitudes of the newly detected earthquakes, we find that an additional 20-25 M 1.0+ events were potentially locatable by the regional network. Additionally,

we find that many of the 90 template events detect new earthquakes across essentially the entire time period examined. Even the least effective template event, a M 1.89 on 1/8/2024, was able to detect new events from 1/2/2022 through 8/9/2024. These results suggest that the template matching method based on single station recording can be a useful complement to network monitoring of earthquake swarms in the eastern USA.

**S3-2** Joint inversion of receiver functions and surface-wave dispersion in the Eastern Tennessee Seismic Zone. **Julia, J.**<sup>1</sup>, V. Levin<sup>1</sup>, C. Chai<sup>2</sup>, M. Maceira<sup>3</sup> (1: CERI, University of Memphis; 2: Oak Ridge National Lab; 3: ORNL)

The Eastern Tennessee Seismic Zone (ETSZ) is an elongated zone of intraplate seismicity located in and around the Valley and Range (VR) province of Eastern Tennessee. Epicentral locations characterize the ETSZ as a 300 km long and 100 km wide zone of diffuse seismicity that follows the trend of the neighboring Appalachian orogen and roughly coincides with the New York-Alabama (NY-AL) aeromagnetic lineament. Seismicity occurs along both sides of the NY-AL lineament down to depths of  $\sim$ 25 km, with a larger concentration of seismic sources to the East. The NY-AL lineament has been imaged by local body-wave tomography - and, to some extent, ambient noise tomography - as separating low velocities to the West from fast velocities to the East. Those studies, however, were limited in their depth extent by either local ETSZ source depths ( $h < 25$  km, body-wave tomography) or period range ( $T < 15$  s, ambient noise tomography). Deeper velocity structure was nonetheless investigated through inversion of teleseismic transfer functions, which extended the velocity separation across the lineament down to Moho depths (40-50 km) and, most puzzlingly, revealed the existence of a 'Moho hole' (a region with no identifiable crust-mantle transition) East of the lineament. Here, we investigate changes in crustal structure across the NY-AL lineament by jointly inverting P-wave receiver functions and surface-wave disper-

sion velocities developed from ambient seismic noise. Receiver functions are obtained through deconvolution of the vertical component from the corresponding radial component, while dispersion is obtained from standard multiple frequency analysis on time-frequency-normalized cross-correlation functions. Preliminary results show that lateral variations in crustal velocity is indeed present in the region and that a crust-mantle transition can be reliably identified at all sites.

**S5-7** Characterizing Decadal Seismicity Patterns of Fault Patches in the Mexico Subduction Zone via Template Matching. **Khalkhali, M.**, M. R. Brudzinski, W. Ventura-Valentin (Miami University)

This study focuses on identifying temporal seismicity patterns in Mexico over a decade to gain a more comprehensive understanding of how fault patches behave over longer time periods in a subduction zone setting. We applied single-station template matching to analyze 250 seismic sequences, each containing at least 10 events, selected from the sequence catalog developed by Ventura-Valentn et al. (2024). Sequences were identified using the Zaliapin and Ben-Zion (2013) method, so we treated each spatially connected sequence as a fault patch. We did not relocate matched events due to limited seismic station coverage but prior work indicates matches are within 1 km of templates. To explore the long-term behavior of these fault patches, we focused on data from two consistently operating stations in the Oaxaca region from 2012 to 2022. We identified four overall temporal patterns: Isolated events primarily limited to the template time frame, Ongoing activity with seismicity occurring almost every month, Episodic activity with flurries of activity and periods of quiescence, and Decaying sequences that follow Omori-type aftershock decay patterns over longer time frames. The Episodic pattern was most common, with ~75% of sequences classified at least level 1, followed by Decaying and Ongoing with ~35%, and Isolated with ~20%. Isolated was more associated with mainshock-

aftershocks and Episodic with swarms. Isolated sequences were geographically scattered, with others concentrated along the coastline. Ongoing sequences were concentrated in regions correlated with areas where geodetically determined coupling is transitioning from high to low, providing some clues to what enables that persistent seismicity. Decaying sequences primarily occurred associated with the M7.4 2012, M8.2 2017, and M7.2 2018 aftershock sequences. Intriguingly, Episodic sequences were only ~10% more likely during slow slip episodes but were 4.3 times more likely during the geodetically determined afterslip periods of those 3 mainshocks.

**S9-2** An Advanced Detection and Relocation Workflow for Characterizing Seismicity Associated with Hydraulic Fracturing in the Eagle Ford Basin, Texas. **Kirchenwitz, J.**, M. R. Brudzinski, K. Mazzio, M. Khalkhali (Miami University)

Unlike many areas of the central United States where induced seismicity has been caused by wastewater disposal, most of the earthquakes in the Eagle Ford Basin in Texas have been related to hydraulic fracturing (HF) wells (Fasola et al., 2019; Fasola & Brudzinski, 2023). This includes some of the largest HF-induced earthquakes in the United States, including M4.7 earthquakes on February 17, 2024 and January 30, 2025 and five events larger than M4 since 2018 in Karnes County. The seismicity rate and magnitude has been increasing despite no commensurate increase in HF activity. The seismicity appears to be associated with the Karnes Trough extensional feature, but the detailed pattern of the seismicity and how it relates to faults and HF operations has not been fully characterized. This study has sought to take advantage of the ~5 years of continuous recordings from the dense (25 km station spacing) seismic network in the area to better detect and locate the seismicity. We have developed a workflow for streamlining the processing that starts with 1) catalog events and phase picks and then performs 2) multistation template matching with automated correlation threshold determination for each template, 3) phase arrival identification

for detected matches using cross correlation with the template and other matches, 4) preliminary location of detected matches using the determined phase arrivals, and 5) double difference relocation of template and matched events using cross-correlation enhanced arrival times and a locally determined 1-D velocity model. This approach reveals more than an order of magnitude increase in the number of detected and located earthquakes. Our preliminary results indicate that the seismicity primarily occurs on a series of steeply dipping northeast-southwest trending normal faults. We also observe individual faults repeatedly active over several years correlated with different hydraulic fracture wells.

**S1-1** New Madrid Seismic Zone Seismicity Patterns over Time and Space. **Langston, C.** and C. A. Powell (University of Memphis)

A byproduct of a new, high-resolution velocity tomography of the New Madrid Seismic Zone is a catalog of 5600 accurately located earthquakes comprising about 87% of the total number of earthquakes contained in the New Madrid catalog for the inversion volume during the time interval of 1997 to 2025. Seismicity is highly clustered in space and show new details on the relationship of the intersections of the North fault-East fault-Northern Reelfoot fault and the Axial fault-Northern Reelfoot fault-Southern Reelfoot fault. The Northern and Southern Reelfoot faults are clearly separated by the cross-cutting Ridgley fault, Cottonwood Grove fault, and an additional inferred fault parallel to the Ridgley and Cottonwood Grove faults. Seismicity at this intersection region is confined to depths less than 8km, displaying a horst-like structure. Seismicity-depth histograms for fault segments of the NMSZ show systematics that suggest that crustal temperature, strength, or pore pressure changes with position away from the Northern/Southern Reelfoot transition with earthquakes as deep as 25 km in the outer regions. 3D Fault models are built from the distribution of seismicity and the temporal evolution of events; moment release is investigated on each segment. It is interesting to note that the

cumulative seismic moment inferred from event magnitudes in the 1997-2025 catalog is equivalent to a single M4.9 event. Two robust temporal trends are seen in the seismicity. There appears to be a doubling of earthquake numbers in the period 2012-2025 compared to 1997-2012 in a period of seismic network stability which argues against present seismicity being aftershocks of the events of 1811-1812. Additionally, there is a clear sinusoidal pattern of numbers of events vs hour of occurrence in a day that most likely is caused by the large diurnal variation of ambient ground noise in the embayment affecting network detection.

**S2-7** Fault activity in CEUS seismic zones: Past focal planes to long-term slip potential. **Levandowski, W.** (Tetra Tech, Inc.)

Stress in the Earth's crust fundamentally controls earthquakes. Focal mechanisms demonstrate that seismogenic stress varies across the central and eastern United States (CEUS), both in terms of relative stress magnitudes which control faulting type and stress regime and principal stress directions. As a result, faults of different orientations are reactivated with different senses of slip in each CEUS intraplate seismic zone. Site-specific stress models are therefore needed to quantify local fault slip potential, winnow paleoseismic targets, or identify candidate faults for historic earthquakes and liquefaction features. Here, inversions of earthquake focal mechanisms determine the state of stress, focal planes, and orientations of optimal and other well-aligned faults in the New Madrid, Wabash Valley, Saline River, Eastern Tennessee, Appalachia/Giles County, South Carolina, Central Virginia, Ramapo, and New England Seismic Zones, plus other representative CEUS regions. These analyses are standardized and presented on a common template, with the aim of making them a useful reference for seismological and seismotectonic studies of all kinds in the CEUS.

**S3-5** Lithologic controls on the Mw5.1 Sparta, NC seismic cycle - microgravity and crustal

stress constraints. **Levandowski, W.** (Tetra Tech, Inc.)

During the 2020 Mw5.1 Sparta earthquake, sinistral-reverse slip reactivated an asymmetric patch of the pre-existing Little River Fault (LRF), creating the first observed surface rupture in the eastern U.S. and an unprecedented opportunity to investigate intraplate fault reactivation. Here, the LRF is imaged with a microGal-precision relative gravity survey, then stress inversions and geomechanical calculations examine relationships between stress and faulting for the mainshock and 16 fore/aftershocks. A prominent gravity high aligned with mapped amphibolite intersects and obliquely under-thrusts the LRF up-dip from the hypocenter, where the coseismic scarp reached its maximum height. The coseismic rupture propagated through the flanking low-density material but arrested against the next high-gravity zones. These patterns suggest that dense, strong lithologies both nucleated the mainshock and controlled LRF segmentation. The LRF and focal planes determined from normalized instability,  $I$ , for 14/16 aftershocks are well aligned for slip under the modern N68E maximum stress and strike-slip to transpressive regime ( $I \geq 0.9$ ). Constraints on active focal planes are then used to develop a seismic cycle model. Interseismic strain accumulation was asymmetric about the seismogenic asperity, leading to asymmetric rupture with more offset east of the hypocenter than west. Aftershocks were bimodal. Those on the higher-slip east side accommodated minor additional slip along the LRF. However, aftershocks on the low-slip west side concentrated along the edge of the coseismic slip volume, which parallels the dominant regional joint orientation but is poorly oriented for slip ( $I = 0.24 \pm 0.08$ ). Instead, the focal planes are highly oblique to that trend. These are interpreted as well-oriented, en echelon faults within a pre-fractured belt. This interpretation contrasts with the typical assumption that active fault orientations can be inferred from planes fit to microseismic hypocenters. The Sparta sequence exemplifies reactivation of favorably oriented ancestral faults, highlighting

the importance of crustal stress constraints to understanding fault-zone behavior.

**S3-3** Mid-crustal earthquakes in eastern Tennessee occur within a volume of layered sheared rock. **Levin, V.**, Jordi Julià Casas, Anuradhapura Mahanama (CERI, University of Memphis)

The Eastern Tennessee Seismic Zone (ESTZ) presents a persistent challenge for both the understanding of intracontinental seismicity and the seismic hazard assessment in Central & Eastern US. Earthquakes occupy a volume, with no obvious focusing on planes that could be related to faults. From above, the volume is largely bound by the 3-5 km deep Appalachian detachment dating back to the assembly of Pangea, and extends approximately half-way through the ~50 km thick crust. Earthquakes deeper than ~15 km, including the  $M=4.1$  May 10, 2025 event, occur exclusively beneath the Valley and Ridge and the easternmost Cumberland Plateau, while more shallow earthquakes take place farther east as well. In map view seismicity is largely aligned with the continent-scale NY-AL magnetic lineament associated with a Proterozoic tectonic boundary; however, identifying any linear trends parallel to the lineament within the diffuse distribution of epicenters would be a challenge. To develop additional insight into the crustal architecture of the ETSZ we use records of teleseismic P waves to build directional gathers of P-to-S converted waves sensitive to vertical gradients in both impedance and seismic anisotropy (a proxy for rock texture). Timing of detected converted waves constrains layered architecture of the crust, while their frequency dependence represents the vertical extent and steepness of detected gradients. Comparing P-to-S converted wave times with S-P times of earthquakes with nominal hypocenters below 15 km we position these earthquakes with respect to structures we detect. We find multiple boundaries with strong anisotropy within the upper ~25 km of the crust, and show evidence for a strong impedance contrast at that depth. Regionally consistent anisotropy likely represents rock deformation along the Appalachian detachment

ment and similar deeper structures. We demonstrate that seismicity takes place within the layered anisotropic part of the crust, and above the newly detected impedance boundary.

**S5-8** Radial Anisotropy beneath the North American Midcontinent. **Li, H.**<sup>1</sup>, X. Yang<sup>1</sup>, B. Herr<sup>2</sup>, B. He<sup>1</sup>, L. Liu<sup>3</sup>, A. S. Goddard<sup>4</sup> (1: Purdue University; 2: Rice University; 3: Chinese Academy of Sciences; 4: Indiana University)

As a relatively stable continental core, the North American midcontinent carries abundant structural signatures of lithospheric modifications due to its long tectonic history. Despite numerous studies in the past decades, the mechanism of its formation and tectonic evolution remains unclear. In this study, we construct radial and azimuthal anisotropy models for the lithosphere beneath the North American midcontinent to understand its structures and their implications on the mechanism of lithospheric modifications. The Rayleigh and Love phase velocity results were obtained from ambient noise cross-correlations of continuous waveforms from 2011 to 2014. We incorporate both USArray and several dense regional arrays to expand data coverage to enhance the model resolution. The phase velocity maps show that Rayleigh and Love waves are relatively slower beneath the Illinois basin for periods up to 60 seconds. In addition to the Illinois basin, the Appalachian Foreland Basin, the Nashville Dome, and the Cincinnati Arch show low phase velocities at 27-40 seconds for Rayleigh waves and 27-50 seconds for Love waves. The differences between Rayleigh and Love wave velocities in the lower crust and the uppermost mantle imply extensive, especially horizontal, structural modifications. We will invert for Vsv and Vsh velocities to produce the radial anisotropy model. In addition, we will combine the radial anisotropy results with published azimuthal anisotropy results, such as from SKS analysis and adjoint tomography, to build a comprehensive view of the lithospheric structure of the North American midcontinent. These results will help us understand the structural modification and dynamic evolution of cratonic litho-

spheres within North America and around the globe.

**S8-10** Multifaceted Drivers and Distributed Fluid Injections Orchestrate Earthquake Swarms beneath the Eastern Himalayan Syntaxis. **Ma, J.**<sup>1</sup>, L. Meng<sup>2</sup>, M. Jiang<sup>1</sup>, H. Zhang<sup>3</sup>, G. Hou<sup>1</sup>, Y. He<sup>1</sup>, L. Li<sup>1</sup>, Z. Li<sup>1</sup>, M.-Y. Cai<sup>1</sup>, Y. Feng<sup>1</sup>, Y. Ai<sup>1</sup>, and L. Ding<sup>3</sup> (1: IGG, Chinese Academy of Sciences; 2: UCLA; 3: ITP, Chinese Academy of Sciences)

Earthquake swarms in high heat flow regions are widely recognized as signatures of hydrothermal activity, yet their driving mechanisms in complex tectonic settings remain elusive. The Eastern Himalayan Syntaxis (EHS), a key segment of the IndiaAsia collision, provides a rare opportunity into faultfluid coupling, though its swarm activity has never been systematically investigated. Leveraging data from a dense seismic array deployed across the EHS between 2023 and 2024, we constructed a high-resolution earthquake catalog containing ~8,500 events, which reveals a wide range of swarm behaviors. Notably, we identify, for the first time in natural settings, the Bianba swarm, which is triggered by distributed fluid injections from multiple sources. In this case, fluid injection initiates seismicity, while the pattern and evolution of distributed fluid-induced activity are governed by the complex 3D fault geometry and variations in fault zone permeability. Yigong swarm exhibits a coupled process: fluid reduces the effective normal stress to trigger earthquakes and simultaneously drives aseismic slip that rapidly migrates across the fault to farther regions. Static stress changes from earlier ruptures within the swarm sequence subsequently promote failure in adjacent areas. This feedback loop operates only with sustained fluid supply and ceases once injection stops. These findings demonstrate that fluid injections and feedback processes, shaped by fault structure, jointly govern swarm dynamics in high heat flow orogenic systems.

**S5-9** Seismic Monitoring and Dynamic Triggering around the Santa Ana Volcanic Complex

in Western El Salvador. **Martinez-Coto, A.**, Navin Thapa, and Thomas H. W. Goebel (CERI, University of Memphis)

In Western El Salvador, the Santa Ana Volcanic Complex is a seismically active region where a complex setup of volcanic systems and local faults presents significant hazards. Its main features include the Coatepeque Caldera and the Santa Ana, Izalco, and Cerro Verde Volcanoes. To advance our understanding of this environment, a seismic network was deployed in late 2023. The network is a collaboration led by the University of Memphis and the University of El Salvador, with key partners that include the Ministries of Environment and Education of El Salvador. By installing seismometers primarily in local schools, the project integrates monitoring and research with the goal of improving community hazard awareness. This work focuses on the development of a workflow to enhance seismic monitoring in the area. We use machine learning phase pickers and associators to automate data processing and catalog creation, resulting in a higher spatial resolution and lower magnitude of completeness than standard catalogs. During the implementation of this workflow, we found clear evidence of dynamic triggering, where the passage of body and surface waves from distant large earthquakes initiated an increase in local seismicity. We observed an essentially instantaneous increase in the local microseismicity rates due to the M7.6 North Honduras event in February 2025. A similar rate increase was also observed following the M8.8 Kamchatka earthquake in July 2025. This is one of the first observations of dynamical triggering in Western El Salvador, demonstrating that the local fault, hydrothermal, and volcanic systems are sensitive to small stress perturbations. We will build on these first results and explore implications for the state of stress and eruption prognostics for the nearby active volcanoes. The success of our enhanced monitoring workflow not only facilitates scientific discoveries but also strengthens the network's capability for early detection and improved hazard assessment in this volcanically active region.

**S8-11** Investigating Human Induced Seismicity in the Eagle Ford Shale Play: Evidence for Hydraulic Fracturing Correlating with Increasing Magnitudes of Seismicity. **Mazzio, K.**<sup>1</sup>, M. Brudzinski<sup>1</sup>, A. Reedy<sup>2</sup>, J. Kirchenwitz<sup>1</sup> (1: Miami University; 2: Fort Valley State University)

The Eagle Ford Shale Play (EFSP) located southeast of San Antonio, Texas has had an increase in the rate and magnitude of earthquakes in recent years (Fasola et al., 2019). The EFSP occurs in an area of low seismic hazard, making naturally occurring seismicity unlikely. Hydraulic fracturing by injecting pressurized fluid to stimulate production of hydrocarbons from unconventional shale layers has enabled the EFSP to become the 3rd largest producer of both oil and natural gas in the US. With several magnitude  $M_w > 4$  earthquakes occurring recently creating increased risks, a reevaluation of the operational activity and its relationship to seismicity is needed. We manually compared well records from FracFocus and earthquake times and locations from TexNet to investigate whether a correlation has persisted in the EFSP since 2019. Fasola et al. (2019) found that 94  $ML \geq 2.0$  earthquakes spatiotemporally correlated to 211 HF well laterals. Our preliminary work has focused on the area around Hobson and Gillett, TX, where a  $M_w 4.5$  occurred in January 2024 and a  $M_w 4.7$  occurred in January 2025. During January 2024 near Hobson, we identified a single well pad with 9 wells listed as active during the seismicity. Seismicity also occurred in this same area in several previous time periods when different nearby HF well pads were active, including during the  $M_w 4.0$  that occurred in September 2023. Our early findings indicate that the increase in number and size of seismicity in the past few years is not due to increased HF activity. The first hypothesis for increased seismicity is that HF well locations could have become more concentrated near active faults despite fewer wells overall. A second hypothesis for increased seismicity would be that HF wells have maintained similar locations but repeated injection has caused underground pore fluid pressure to increase making seismicity more likely. Our

preliminary results suggest the second hypothesis is more likely given that we have seen increasing seismicity in both the Hobson and Gillett regions despite no increase in the HF activity. A parallel study is also investigating the detailed locations of seismicity in this area using double difference relocation of microseismicity revealed by template matching, which indicates the seismicity is likely occurring on pre-existing normal faults. Our goal is to integrate this work with previous and concurrent findings to produce an enhanced understanding of the causes of seismicity in the EFSP that will serve as guidance for potential regulation to mitigate risks from operational activity.

**S2-8** Waveform Analysis of Three Earthquakes in 2021, Baltimore County, MD. **McLaughlin, K.** (Self)

The waveforms of three shallow earthquakes 25, 27 June and 15 August 2021 in Baltimore County, MD were studied. Eighteen Raspberry Shakes were operating within 96 km (and 8 between 9 to 50 km) in this sparsely monitored Baltimore suburban area a few km above the Piedmont Coastal Plain physiographic fall-line boundary. These amateur scientist stations afforded a detailed study not available given the standard professional network (closest station 19 km). Waveform correlations at multiple stations and S-P differences observed at a distance of 9 km indicate the three events were tightly clustered. A joint solution was found that localized all events within an error ellipse. The smallest event is within 0.7 km of the two larger. A focal mechanism from 5 shakes and one standard network station was found with NE-SW P axis and near vertical B axis. Analysis of the 1-3 Hz Rg surface waves propagating in the Piedmont metamorphics infers depths as shallow as 1 km. Spectral analysis of the three events estimates Mw of 3.0, 2.4 and 2.1, corner frequencies of 7, 19, and 37 Hz and a stress drops of each of 1 MPa. The largest two events are within 100 m and may represent the same asperity which would have radii less than 300 and 200 m respectively based on standard source scaling of

moments and corner frequencies.

**S9-4** Seismic Analyses of Quarry Blasts in NW Miami, Florida, 2019-2025. **McNutt, S.** (University of South Florida)

Quarry blasting is conducted in NW Miami to mine aggregate for the construction industry. The upper layer of limestone is mined using ripple blasting with charges of up to about 50,000 lbs of explosives. We installed a network of 6 seismic stations in July 2019 and to date have recorded 3750 blasts. The instruments are three Raspberry Shake 3-component seismometers and three Raspberry Shake vertical seismometers plus infrasound sensors. The network aperture is about 10 km. The blasts occur in at least six different mines. Blasting is done between 8 a.m. and 4 p.m. (local) Monday through Friday. Many of the blasts are felt by local residents as both seismic shaking and airwaves that are heard as well as causing air-coupled shaking. The local residents have been concerned over the possibility of shaking causing damage to homes. The seismic waves are 8-10 Hz P waves initially and 1-3 Hz Rayleigh waves dominating the later parts of the seismograms. S waves are observed in some cases, presumably as a result of the ripple blasting. The largest blasts have magnitudes of  $M \sim 3$  although  $\log A_0$  values are not well known. Cultural noise is high in Miami, but there are no natural sources of seismicity nearby, so blast signals stand out clearly. The top layer is overburden (muck)  $\sim 2$  m thick. The mined unit is the Miami limestone directly under the muck. It is  $\sim 28$  m thick and has a  $V_p$  of about 2.7 km/sec. The underlying unit has  $V_p > 4$  km/s. In January 2025 the mines changed strategy and began to use smaller charges more often. Monthly total numbers of blasts went from 50-60/month to 77-109/month. We infer that this allowed the same total amount of rock to be mined but individual blasts were smaller and less likely to be felt strongly.

**S7-3** Constructing an Intensity Prediction Equation as a Step Toward Characterizing Site Amplification with DYFI Data. **Meyer, E.<sup>1</sup>**,

L. G. Baise<sup>1</sup>, M. Roberts<sup>1</sup>, S. Nie<sup>1</sup>, and J. Kaklamanos<sup>2</sup> (1: Tufts University; 2: Merrimack College)

Understanding and quantifying site amplification in the Central and Eastern United States (CEUS) remains a challenge. Sparse seismic station coverage, with many instruments placed on rock, makes it difficult to observe amplification effects and incorporate them into ground-motion models. Macroseismic intensity data from the Did You Feel It? (DYFI) program provide an opportunity to supplement traditional ground motion recordings by offering dense coverage across both geologic and population gradients, revealing patterns that stations alone cannot. Our work aims to use DYFI observations to explore spatially variable site amplification across the CEUS. We find that current Intensity Prediction Equations (IPEs), exhibit biases with respect to magnitude, distance, and spatial distribution. By leveraging the vast volume of DYFI reports, we first unbias these trends, with the eventual goal of recovering regional and local amplification patterns using mixed effects regression. To do this, we build a macroseismic dataset from the last 25 years of DYFI data and use this to fit a new, unbiased IPE. By treating DYFI data as more than anecdotal reporting, we can leverage its richness to better understand and model how spatial variability in site amplification shapes seismic hazard.

**S5-10** Comparison of 2D, 2.5D and 3D Electric Resistivity model in detecting shallow sub surface faulting. Mitra, I.<sup>1</sup>, R.T. Cox<sup>1</sup>, M.H.Loke<sup>2</sup>, K. Karki<sup>1</sup>, S. Islam<sup>1</sup>, C.H. Cramer<sup>1</sup> (1: University of Memphis; 2: Geotomo Software)

Shallow active faults are 3D geological structures that hold information about neotectonic framework of the region, and 1D or 2D electrical resistivity (ER) surveys are insufficient to provide a complete picture of subsurface structure, whereas 3D ER is a relatively easy method to investigate shallow faults but has not been widely applied for this use. The broader implication is to demonstrate the application of 3D ER sur-

vey in characterizing fault zones and to establish the effectiveness of 3D ER survey. For comparison to a Quaternary documented fault, the survey was conducted in Lauderdale, TN along the Eastern Reelfoot Rift Margin (ERRM) at Porter Gap, the northernmost paleoseismic trench site previously on the eastern Reelfoot Rift margin (ERRM). Sixteen fault-parallel lines of 28 m length with 2 m electrode spacing were chosen for the study. The ER survey was performed using Advanced Geoscience Inc.(AGI) Supersting R8 to image subsurface faulting using dipole-dipole array configuration. These 2D surveys were combined in EarthImager 3D and then subjected to inversion to make 2.5D model. Model was updated by solving linearized inversion problem to minimize data misfit. The maximum vertical depth of 2.5D model is 11.9 m that shows near-vertical fault cutting paleochannels and revealing vertical offset of ~4 m. The 2.5 D generated model agrees with observations of this fault in trench excavations and provides a magnitude of vertical slip previously unobserved. A true 3D model generated using RESINV64 software has 20m of maximum depth of investigation. Both the 2.5D and 3D models suggest a >48 right-lateral fault offset.

**S5-11** Enhanced earthquake detection in Snyder, Texas using LOC-FLOW with dense SmartSolo deployment and TexNet stations. Montazeri, S.<sup>1</sup>, X. Chen<sup>1</sup>, L. Arthur<sup>1</sup>, H. Deshon<sup>2</sup>, Jay Tung<sup>3</sup> (1: Texas A&M University; 2: Southern Methodist University; 3: Texas Tech University)

Earthquake activity in the Snyder, Texas area has increased in recent years, motivating dense monitoring that complements the statewide TexNet backbone network. Following the 2024 M5 Snyder earthquake, a nodal array was deployed near Snyder. The open workflow LOC-FLOW was applied to a combined dataset with the 12 temporary 3-component SmartSolo nodes and 4 nearby TexNet stations. TexNet provides statewide coverage and rapid cataloging and has lowered the magnitude of completeness in key Texas regions, enabling detailed lo-

cal studies such as this one. Waveforms from 2024/10/05 to 2024/11/30 were preprocessed (demean, detrend, taper, merge) and resampled to 100 Hz. Detection and picking used PhaseNet, association used REAL, and initial absolute locations were obtained with HYPOINVERSE within the LOC-FLOW framework; quality control included multi-station phase coherence and time-windowed visual review. We then compared detections against the public TexNet catalog for the same period. The workflow yielded more than 500 candidate earthquakes in the study window. All 47 TexNet-reported events in the area were recovered by our workflow, with median detectioncatalog origin-time differences of  $\sim 0.7$  s (range  $\approx 0.11.4$  s) and consistent PS phase timing across the network. Daily rates peaked at  $>40$  events/day in late October, with additional low-magnitude events evident on the nodal array that are weak on the sparse permanent network but show coherent phases on 12 SmartSolo stations and up to 4 TexNet stations. These results demonstrate that combining LOC-FLOW with a temporary dense array can (1) capture low-magnitude local events missed by regional catalogs, (2) provide high-quality phase sets for relative relocation (HypoDD/GrowClust), and (3) establish a vetted baseline for future ground-motion and swarm/cluster analyses in West Texas. While TexNet provides critical regional coverage, the SmartSolo deployment reveals that additional earthquakes were not reported in the TexNet catalog. By integrating both networks, we produce a more accurate local earthquake catalog for the Snyder region.

**S8-14** Tracing Tennessee Tremors, the Construction of a Historic Seismicity Map for the State of Tennessee. **Moran, N.<sup>1</sup>**, William Jackson<sup>2</sup>, Valerie Harrison<sup>2</sup>, Maxwell O’Hearn<sup>3</sup> (1: CERI, University of Memphis; 2: Tennessee Geological Survey; 3: University of Memphis)

One of the ways to display historic seismicity for use by the public and government officials is by plotting historic earthquake epicenters on a map. This provides a vivid graphic rep-

resentation of where seismic activity is located across the state. In developing the map several issues of historic catalog accuracy have arisen that show that historic data can both illuminate and obscure where these historic events have occurred. Modern researchers seeking to develop these maps for their own states need to be aware of these issues in making them. An approach that incorporates historic data in a useful way is needed to refine the data for these maps taking into account old records and modern data searches that might uncover seismic events of importance that were not noticeable in previous research.

**S9-1** Interplay of Wastewater Injection and Hydraulic Fracturing in Induced Seismicity near Kingfisher, Oklahoma (20192024). **Ogvari, P.**, J. Walter, H. Xiao, I. Woelfel, A. Thiel, N. Gregg, B. Mace (Oklahoma Geological Survey)

Hydraulic fracturing in Oklahoma is commonly linked to small earthquakes ( $M < 2$ ), but can also produce larger, felt events. The hydraulic fracturing process often occurs in regions with long-term subsurface wastewater disposal. Although hydraulic fracturing and wastewater disposal target different geological formations, their combined impact on induced seismicity can be cumulative, with respect to subsurface stresses. This study investigates how wastewater injection and hydraulic fracturing interact to influence seismicity near Kingfisher, Oklahoma, from 2019 to 2024. Analysis of the Oklahoma Geological Survey (OGS) earthquake catalog and injection data indicates that seismicity began about 5 km northeast of the injection point on a previously inactive fault in mid-2019, during concurrent fracturing and injection at relatively high disposal wellhead pressures ( $>8$  MPa). The earthquakes are located beneath four hydraulic fracturing wells whose horizontal sections intersect the seismogenic fault. After injection was paused by a regulatory inquiry, well pressures dropped below 4 MPa, and the rate of earthquakes associated with hydraulic fracturing declined, with only six events of  $M > 2.5$  recorded compared to 20 in the previous pe-

riod. We enhance the OGS catalog by detecting smaller earthquakes using the network-based matched filter technique and refine subsequent new earthquake locations with hypoDD to improve the spatiotemporal resolution. We will present updated results to illustrate the evolution of earthquakes along the seismogenic fault. Additionally, we will model stress changes on the fault from multiple well injections to quantify the approximate the relative stress change over the study period. This will help analyze the potential for wastewater injection to trigger seismicity between 2020 and 2024, in the absence of concurrent hydraulic fracturing. This project has the potential to inform future studies focused on the interplay between two different kinds of induced seismicity adjacent to one another.

**S8-6** Investigation of the Subsurface Structure of the Chestnut Hill Reservoir Earth Embankment Dam Using Ground Penetrating Radar (GPR). **Olawoyin, V.**, J. E. Ebel, E. Petschek (Boston College)

The Chestnut Hill Reservoir earth embankment dam, constructed between 1866 and 1870, represents critical infrastructure in Boston's water management system. Classified as a high hazard potential dam by the National Inventory of Dams, comprehensive understanding of its subsurface structure is essential for safety assessment and long-term maintenance planning. This study employed Ground Penetrating Radar (GPR) technology to conduct a non-invasive geophysical investigation of the dam's internal features, utilizing a GSSI SIR 3000 system with 270 MHz antennas to collect high-resolution subsurface profiles along approximately 1.2 kilometers of survey lines along the top of the dam. The GPR investigation successfully imaged subsurface features to depths of approximately 3.5 meters, revealing previously undocumented structural elements critical to understanding the dam's construction and integrity. The study identified extensive vaulted chambers beneath Effluent Gate House 1, characterized by distinctive hyperbolic reflection patterns indicating brick arch construction approximately

2 feet thick. These chambers, validated through comparison with historical architectural drawings from 1870 but had been absent from later documentation spanning 1995-2015. Additional key findings include identification of the clay core zone within the dam, which is known from historical records, with horizontal reflectors appearing at elevations and dimensions consistent with 19th-century engineering specifications. The investigation identified water pipe infrastructure at depths of 2-2.5 meters, including the 48-inch blow-off pipe bedded with crushed stone that was repaired after seepage issues in 2019. Cross-validation through multiple parallel profiles confirmed the repeatability and reliability of feature detection, with structural elements consistently identified across survey lines, suggesting good overall imaging of the substructure of the 155-year-old dam.

**S5-12** Referenced Empirical Ground-Motion Models for Arias Intensity, Cumulative Absolute Velocity, and Significant Durations for the Alborz Region of Northern Iran. **Pakniat, S.**, S. Pezeshk, M. Davatgari-Tafreshi (University of Memphis)

In this study, we have developed new Ground Motion Models (GMMs) to estimate significant durations (D5-75 and D5-95), Arias intensity (IA), and cumulative absolute velocity (CAV) based on the dataset from the Alborz region of northern Iran by utilizing the referenced empirical method (REM) introduced by Atkinson (2008). We used D5-75 and D5-95, developed by Sandkkaya and Akkar (2017), and IA and CAV, developed by Campbell and Bozorgnia (2019), as reference ground motion models. The residuals are calculated as the differences between the logarithm of observed significant durations and those from Sandkkaya and Akkar's (2017) reference GMMs, and the differences in the logarithm of observed IA and CAV and those from Campbell and Bozorgnia's (2019) reference GMMs. We used a mixed-effects regression to adjust the Sandkkaya and Akkar (2017) and the Campbell and Bozorgnia (2019) GMMs for use in the Alborz region of Iran. We developed a simplified

functional form as a function of Mw, Rjb, and VS30. The reliability of the proposed GMMs has been evaluated through a comparison with observed data, previous GMMs, and residual analyses. The residual analyses indicate no significant bias or trend as a function of Mw, VS30, and Rjb, in both between-event and between-station corrected residual components, as well as event-site corrected residual components. The dataset comprises 775 acceleration records from 167 earthquakes, recorded at 309 stations between 1976 and 2020, with a Joyner-Boore distance (Rjb) range of  $1 \text{ km} < \text{Rjb} < 160 \text{ km}$  and a moment magnitude (Mw) range of  $3.0 \leq \text{Mw} \leq 7.4$ , respectively.

**S2-9** Characterization of the 2024 Mw 4.8 Tewksbury, NJ Earthquake Fault Plane Geometry using Relocated Aftershocks. **Petschek, E., J. E. Ebel** (Boston College)

In April 2024, a Mw 4.8 earthquake occurred in Tewksbury, New Jersey. Situated roughly 70 km from New York City and 80 km from Philadelphia, the event caused minor damage in both cities and was felt throughout the northeastern United States. Over 200 aftershocks were generated by the 2024 M4.8 Tewksbury mainshock, providing an opportunity to characterize the geometry of the host fault or faults. By relocating aftershocks via relative locations, a high-resolution spatial distribution of hypocenters can be assembled and used to delineate subsurface fault planes. It was determined that, after finding all possible P- and S-wave arrival times at stations between 30 km and 190 km of the mainshock, a few dozen aftershocks were recorded on a sufficient distribution of regional seismic network stations to be used in a relative location analysis. For many of the events in the relocation process, the P-waves of nearby events frequently have weak cross-correlations, whereas the S-waves typically have strong cross-correlations. This discrepancy between P and S cross-correlations is in contrast to relative location analyses in other studies, where strong P-wave cross-correlations were found. Of the events analyzed so far for which high-resolution

relative locations were found, the relocated aftershocks of the Tewksbury earthquake form a flat surface resembling a fault plane with a northwest strike and a southwest dip of roughly 45 degrees. These relative locations suggest that earthquake activity following the Tewksbury mainshock occurred on a relatively simple fault plane.

**S1-3** New Velocity and Fault Structure Analysis of the New Madrid Seismic Zone. **Powell, C., C.A. Langston** (University of Memphis)

New detailed P- and S-wave velocity ( $V_p$  and  $V_s$ ) models and hypocenter relocations for the New Madrid seismic zone (NMSZ) reveal interesting relationships between major velocity anomalies, the presence of an axial intrusion, and hypocenter distributions. The velocity models and hypocenter relocations are determined using local earthquake tomography based on arrival time data in the Cooperative New Madrid seismic network catalog for the period January 1, 1997, through July 5, 2025. The dataset consists of 5,609 earthquakes, 93,338 P-wave phases and 66,333 S-wave phases recorded at 59 stations. Major velocity anomalies are associated with the Northern Reelfoot and Axial faults. An important relationship exists between the alkalic Reelfoot intrusion and the hypocenters. Northern Reelfoot fault earthquakes in the depth range 4.65–6.65 km occur along the steep northeastern edge of the intrusion and deeper earthquakes occur within the intrusion in a high  $V_p/V_s$  ratio region indicative of high pore pressure. The Southern Reelfoot fault occurs in a portion of the intrusion with low magnetic intensity and is cut by northeast trending faults including the Axial, Cottonwood Grove and Ridgely faults. Three-dimensional views of the seismicity and planes fit to the hypocenters indicate that the Southern and Northern Reelfoot faults contain numerous northeast trending faults, in agreement with a recent focal mechanism study. We suggest that both strike-slip and reverse motion occur on the Reelfoot fault during large earthquakes. An obvious decrease in seismicity occurs at the southern end of the Northern Reelfoot fault. This fault segment is associated with the Tiptonville

Dome, the highest elevation associated with vertical motion on the fault and the location of the large 1812 earthquake. We suggest that this portion of the fault may be locked, posing increased seismic hazard.

**S6-1** Comparative analysis of background seismicity rate estimates and their uncertainties in tectonic and volcanic environments. **Rinty, S.**, THW Goebel (University of Memphis)

Estimating background seismicity rates and understanding potential temporal changes is crucial for the reliable probabilistic seismic hazard assessment. The accuracy of background seismicity rate estimates depends on the quality and consistency of the underlying seismicity catalogs and the ability to resolve the spatial-temporal clustering of earthquakes. Here, we compare the performance of three approaches, i.e., Reasenberg declustering, Gamma distribution fit, and Nearest Neighbor Distance. We analyze the three methods in volcanically active Hawaii, tectonic Southern California, and stochastic ETAS simulations with short and long-term rate variations. We find Reasenberg and Nearest Neighbor provide almost similar rates in Southern California, but in Hawaii Reasenberg does not resolve any eruption effects on the background rate. Nearest Neighbor and Gamma show a significant background rate increase during the 2018 eruption, followed by a sustained elevated rate thereafter. Stochastic ETAS-based catalogs show Nearest Neighbor performs better in resolving transient rate changes, for both intermediate and short-term variation. Gamma distribution fits underestimate rates over the long-term but substantially overestimate background rates during large events with M 6. Reasenberg performs well in southern California but overestimates rates in ETAS catalogs, revealing the limitation of spatially specific parameter tuning. Our analysis using nearest neighbor highlights the difference in clustering characteristics between volcanic and tectonic seismicity. Seismicity during and after eruptions in Hawaii are more clustered in space and time than expected for standard triggering processes in ETAS and southern Cal-

ifornia. Short term eruptive processes like dyke intrusion and hydro-thermal fluid movement can lead to failure of pre-stressed faults, resulting in increased seismicity within a short time. Such seismicity may generate densely clustered mode with small inter-event times. Long-term volcanic processes, e.g., cyclical inflation and deflation of magma reservoirs, can result in stress change over time, leading to increased background seismicity. The susceptibility of background seismicity to long-term eruptive processes is supported by the rate increase after the 2018 eruption.

**S8-7** The 20 June 2025 Mw 4.9 Event in the Central Alborz, Iran: A Rare Tectonic Normal-Oblique Faulting Earthquake within a Complex Transpressional Regime. **Rodriguez-Cardozo, F.**<sup>1</sup>, J. Braumiller<sup>1</sup>, C. Tape<sup>2</sup>, A. Ghods<sup>3</sup>, J. Hu<sup>4</sup>, S. Pham<sup>4</sup>, J. Thurin<sup>2</sup>, H. Tkali<sup>4</sup> (1: University of South Florida; 2: University of Alaska in Fairbanks; 3: Institute for Advanced Studies in Basic Sciences; 4: Australian National University)

On 20 June 2025, a Mw 4.9 earthquake struck the central Alborz Mountains in northern Iran. Using high-quality broadband seismic stations, we performed a full moment tensor inversion, employing different estimation approaches with different subsets of data. All approaches yielded a double-couple oblique-normal faulting solution at 7 km depth. This event is anomalous for the region, as the Alborz accommodates deformation primarily through thrust and left-lateral strike-slip faulting within a complex transpressional regime. The earthquake is the first significant normal faulting event in central Alborz in 37 years. While rare, extensional tectonism can arise in transpressional settings where strain partitioning can occur due to structural anisotropy and fault zone geometry. The seismological evidence supports previous geological observations and geodynamic models that have proposed localized transtension in the active central Alborz. Since this earthquake occurred in the context of increasing hostilities in the Middle East, our moment tensor analysis also served as a screening process for avoiding the spread of misinformation

as our results demonstrate the tectonic nature of the event.

**S2-10** Probing Crustal Structure Across the Central United States Using P-to-S Converted Receiver Functions and Teleseismic P-wave Coda Autocorrelograms. **Soni, Y.<sup>1</sup>** and N. Seth Carpenter<sup>2</sup> (1: Baylor University; 2: Kentucky Geological Survey, University of Kentucky)

Previous studies have reported that the crust beneath much of the central and southeastern Illinois Basin is anomalously thick compared to surrounding regions of the North American Mid-continent. Imaging results reveal pronounced lateral variations in crustal thickness, with the Moho reaching depths of  $\sim$ 5062 km, particularly beneath the Sparta Shelf region. Multiple hypotheses have been proposed to explain this thick crust, including inherited crustal features from North American accretion, shallow under-thrusting or shortening during convergent margin tectonics. Together, these results highlight that the Illinois Basin represents a complex, heterogeneous cratonic region where both ancient tectonic processes and more recent structural modifications have strongly influenced crustal architecture. We investigate the crustal structure beneath Illinois, Indiana, and Kentucky using broadband seismic data from the Ozark-Illinois-Indiana-Kentucky (OIINK) Flexible Array and the nearby Central and Eastern United States Network (CEUSN, N4). We compute P-to-S receiver functions and teleseismic P-wave coda autocorrelations to probe crustal discontinuities and velocity variations. Event gatherers from both data functionals are analyzed as a function of ray parameter to constrain Moho depth, and we assess how teleseismic autocorrelations complement receiver function results. To evaluate the reliability of extracted reflections using teleseismic P wave coda autocorrelograms, we employed a velocity analysis method akin to semblance analysis in exploration seismology. This procedure helps identify reliable P-wave reflections and determine appropriate data processing parameters. Phase-weighted velocity analysis is applied to both datasets to highlight

crustal phases, followed by moveout correction and phase-weighted stacking to enhance coherent arrivals. Finally, the resulting receiver functions and autocorrelations are then jointly inverted to obtain detailed constraints on crustal thickness and velocity structure. By integrating these complementary approaches, we reveal new aspects of the heterogeneous crustal architecture of the central United States, with implications for the tectonic evolution of the North American Craton.

**S5-13** Investigating Potential Relationships Between Rates of Seismicity, Strain Accumulation, and Slow Slip in the Oaxaca Region of Mexico. **Szucs, E.<sup>1</sup>**, M. R. Brudzinski<sup>1</sup>, S. Graham<sup>2</sup>, E. Cabral-Cano<sup>3</sup>, W. Ventura-Valentin<sup>4</sup>, M. Khalkhali<sup>1</sup> (1: Miami University; 2: The College of New Jersey; 3: Universidad Nacional Autnoma de Mxico; 4: Southern Indiana University)

Recent research has suggested that seismicity may be more likely during slow slip episodes (SSEs). If this relationship can be quantified, it would be an important factor to build into operational earthquake forecasting. The Mexico subduction zone is an ideal location for studying the interaction between SSEs and earthquakes due to the region's frequent seismic activity and well documented SSEs. In fact, there were notably ten magnitude 7 or larger earthquakes from 2012 to 2022. In addition to SSEs, GNSS time series data from southern Mexico has revealed an intriguing variation in the rate of strain accumulation associated with subduction in between SSEs. Analyzing GNSS data from an inland and a coastal station in the Oaxaca region from the years 2004-2021, we compared the geodetic rates of motion with estimates of the seismicity rate in neighboring regions over the same time frames. In comparing over 30 different sets of geodetic and seismic observations, our results indicate that there are no strong relationships between either the rate of slow slip or the rate of strain accumulation with the concurrent seismicity rate. The strongest correlation we did observe was a weak relationship demonstrating that SSEs with a shallower depth tend to have a higher normal-

ized earthquake rate for the coastal region. We found stronger relationships when we just considered geodetic relationships, with the strongest being that SSEs at the inland site with a higher average slip rate tended to have shorter duration, implying a fairly constant slow slip release.

**S8-13** Identification of Tornado Seismic Signals (TSS) in the Central United States. **Thompson, S.<sup>1</sup>**, N.S. Carpenter<sup>1</sup>, Y. Suni<sup>2</sup>, Z. Wang<sup>3</sup>, E.W. Woolery<sup>3</sup> (1: University of Kentucky; 2: Baylor University; 3: Kentucky Geological Survey)

Tornadoes cause extensive property damage and endanger lives. While Doppler radar can indicate tornado potential, it cannot confirm when one is on the ground unless radar reflections detect lofted debris. Once a tornado touches down, its energy can be transferred into the earth as seismic vibrations; thus, on-the-ground tornadoes may be detectable by seismometers. Previous studies have not agreed on a characteristic TSS frequency range and have presented only limited analyses of TSS generation mechanisms, wave types, and attenuation. Recently, two EF-4 tornadoes touched down in the central United States one on December 10, 2021, which traveled 129 km from NE Arkansas into NW Tennessee, and another on May 16, 2025, which traveled 97 kilometers through south-central Kentucky. Each tornado passed within 2 km of a broadband seismic station, motivating new TSS investigations. In this study, we identified likely TSS in continuous broadband data using meteorological data from the National Weather Service. Initial observations reveal that TSS waveform amplitudes generally increase as the tornado approaches, peak when the tornado is closest, and decrease as the tornado departs. Spectrograms and filtered seismograms show strong energy bands from 0.0015 Hz during the tornado's closest approach, with the 13 Hz range showing the most consistent correlation with tornado proximity. Initial wave-type characterization of the December 2021 tornado from particle motion diagrams reveals that radial- and transverse-vertical motion in the 13 Hz band is mostly

elliptical to semi-elliptical during the tornado's approach and departure and primarily vertical when the tornado is closest. Here, we present TSS observations as well as the results of quantitative polarization analyses, which we are using to further evaluate wave types, signal coherence, and source directionality. We also present correlated pressure and infrasound data acquired during the May 16, 2025, tornado using sensors collocated with the seismometer.

**SM-1** When the Earth Quakes: Father James B. Macelwane and the Institute of Technology. **Waide, J.** (Archivist Emeritus, Saint Louis University)

**S2-11** Re-analyzing Eastern North America Seismic Archives to Study Seismogenic Processes and Improve Seismic Monitoring. **Waldhauser, F.<sup>1</sup>**, E. Beauché<sup>1</sup>, W.-Y. Kim<sup>1</sup>, D. Schaff<sup>1</sup>, K. Wang<sup>2</sup>, W. Zhu<sup>3</sup> (1: Columbia University; 2: Chinese Academy of Sciences; 3: UC Berkeley)

The Lamont Cooperative Seismic Network (LCSN) has been recording earthquakes in the northeastern United States for decades until 2020 when funding cuts resulted in deteriorating network and operation performance. Efforts in reviving the network are ongoing, and from a total of 44 operating stations during its peak times LCSN now has 21 stations reliably recording seismic events, with an additional 10 stations slated for repair this year. We are setting LCSN up as a seismic network for research and education with the goal to improve our understanding of earthquake occurrence, the nature of active faults, and the hazards they impose in this stable continental region (SCR). A recently NSF-funded cooperative project between Lamont and UC Berkeley aims at reanalyzing the entire continuous LCSN waveform archives and those of neighboring networks in eastern North America by applying supervised machine learning (ML) and template matching for event detection, unsupervised ML for source characterization and discrimination, and cross-correlation and double-difference methods for precise event location. We

present first results from combining these tools in computational workflows that efficiently handle massive amounts of data. We are developing a deep-learning phase picker optimized specifically for monitoring regional-distance earthquakes in the eastern U.S. using recordings of the recent 2024 Mw4.8 Tewksbury earthquake. From an initial, large-scale re-analysis of 20 years of the LCSN archive we find about 10 times more earthquakes than in existing catalogs. We will use these new data to gain fundamental new insight into SCR seismogenesis and seismotectonics at a broad range of spatial scales. The new processing and analysis workflows will be become an integral part of a novel model for efficient network operation and seismic monitoring.

**S1-2** Solid earth tides have a stronger effect than seasonal water loading on earthquake modulation in the New Madrid Seismic Zone. **Walter, J.<sup>1</sup>, H. DeShon<sup>2</sup>, P. Neupane<sup>2</sup>** (1: Oklahoma Geological Survey; 2: Southern Methodist University)

The New Madrid Seismic Zone (NMSZ) in the central United States has long been an enigma for earthquake seismologists and the subject of considerable debate regarding ongoing seismic hazard. We utilized a deep-learning picker workflow to enhance the seismic catalog in the NMSZ for a dataset spanning 2012-2021. This time period was selected because continuous data from short-period analog sensors began archiving then, and several non-telemetered FlexArray experiments were deployed across the region during Transportable Array operations. We applied easyQuake (<https://github.com/jakewalter/easyQuake>), a flexible set of tools for detecting earthquakes with deep-learning pickers and locating newly identified events. We identified several challenges with directly using automatic catalogs for analysis due to intermittent station gaps, particularly from the short-period, radio-linked analog stations. When left uncorrected, these stream gaps produced false-positive event identifications. Mitigating these and other issues reduced the catalog by 14%. Within the re-

gion confined to the Reelfoot Rift and other seismotectonic features, we produced a high-quality catalog of 6,105 events, compared to 2,667 events in the CERI catalog over the same period. Relocation of these events highlights several hallmark seismotectonic features of the NMSZ. With this enhanced catalog, we examined hypotheses focused on stress triggering in the NMSZ. A recent study suggested that seasonal water loading in the critical zone and surface modulates earthquake activity, such that reduced water loading in summer and fall promotes microseismicity, while heavy spring rains suppress it (Craig et al., 2017). We also applied a recent formulation by Beauce et al. (2023), which identified tidal triggering prior to the Ridgecrest earthquake, to estimate tidal loading that may contribute to earthquake activity. Because the NMSZ lies intraplate, far from tectonic stress influences near plate margins, it may be especially sensitive to subtle Coulomb stress loads from solid Earth tides or water loading. While the enhanced catalog exhibits several interesting results, also expanding the catalog backward in time to overlap with the Craig et al. (2017) study period and relying solely on the CERI catalog, we found distinct intervals of enhanced tidal sensitivity, with values exceeding the 95th percentile threshold during ~15% of the analysis period. In general, these intervals of tidal phase modulation coincide with reduced seismic activity. Moreover, although seasonal water loading contributes to stress modulation, solid Earth tidal loading appears to be an order of magnitude stronger. The observed weak tidal loading during certain periods presents a perplexing challenge when interpreting these subtle effects, particularly when assessing their importance for understanding the time-evolving seismic hazard in the NMSZ.

**SB-1** The Great Tornado of 1925. **Wiegenstein, S.** (Author)

A hundred years ago, the deadliest tornado in American history originated in southern Missouri. Now known as the Tri-State Tornado, the storm originated near Ellington and swept through southeast Missouri before crossing into

Illinois and Indiana. The devastation of the Tri-State Tornado revealed flaws in the nations storm forecasting and reporting system that grew out of a lack of coordination and a misplaced desire to avoid public panic, flaws that took decades to correct. This presentation uses contemporary accounts and images to re-create Missouri's portion of "the forgotten storm."

**S1-5** Beyond New Madrid: Seismicity of Missouri. **Woods, M.**<sup>1</sup>, H.A.A. Ghalib<sup>2</sup>, and Y. Wang<sup>2</sup> (1: AFTAC; 2: EMR Solutions & Technology)

Since the installation of a network of short-period seismometers in 1974 surrounding the New Madrid region, thousands of small to moderate-sized earthquakes have been cataloged there, and in the Wabash Valley seismic zone. Other than in Oklahoma, where waste injection has fueled intense seismic activity, the rest of the central United States has been thought to be relatively quiescent. But application of modern, automatic workflows (e.g., QuakeFlow & BPMF) to data recorded during the Transportable Array (TA) campaign appears to substantiate a continuing but sparse, broad distribution of earthquakes across the mid-continent as cataloged by Nuttli and Brill (1981). For example, preliminary results using QuakeFlow with TA data from 2011 detected a total of 2024 events in the study region, with magnitudes as small as 0.4, whereas the USGS listed only 957 events, with magnitudes varying from about 1.4 to 5.7. In both cases, most of the events were concentrated around either New Madrid or Greenbriar, Arkansas, but many occurred outside those zones. Moreover, those epicenters are generally consistent with mapped geologic faults and structures, such as the Chesapeake and Bolivar-Mansfield fault complexes in southwest Missouri. Work is continuing to verify the events and to refine their epicenters and magnitudes.

**SM-3** The Role of Seismologists in National Defense. **Woods, M.** (Geophysicist, Air Force Technical Applications Center)

Earlier this year the Seismological Society of America issued a policy statement Protecting Lives, Infrastructure, and Country: Statement on the Importance of Seismic Research and Monitoring for National Defense. This statement highlighted the many ways in which seismological techniques can be employed for National Defense and called for continued funding of research that enables such employment. Among these efforts are seismic hazard monitoring, helping ensure the security of U.S. borders, and providing information about terrorist attacks and major accidents across the globe. The United States has long recognized the need for such applications and has, for decades, sought advice regarding them from the seismological community. The principal seismic application, however, has been monitoring compliance with treaties that limit or ban nuclear weapons tests, and it was this mission that triggered the VELA Uniform program, which helped seismology develop into the rich field we find today. This presentation will sketch the history of that development, focusing on three principal lines of effort, and will highlight contributions by several seismological advisory groups.

**S3-1** Unveiling Shear Velocity Anomalies in the Central Midcontinent of the United States through High-Resolution Joint Inversion: Links to Failed Rifting, Crustal Underplating, and Trans-Crustal Faulting. **Xiao, H.**<sup>1</sup>, S. Marshak<sup>2</sup>, X. Song<sup>3</sup> (1: University of Oklahoma; 2: University of Illinois Urbana-Champaign; 3: Peking University)

The central Midcontinent of the United States is characterized by its low elevation and gentle relief on top of the cratonic platform. This region displays many epeirogenic structures such as basins, domes, faults, and monoclines that formed during Phanerozoic intraplate deformation events. Previous studies have identified significant Moho depth variations in the central midcontinent, which greatly exceeding surface elevation changes or the relief of the Great Unconformity. The most recent major tectonic events in the region were episodes of

failed rifting events and the Grenville orogeny to the east. This work expands on previous research by investigating shear velocity model of the crust and uppermost mantle in this area. We used a joint inversion method that incorporates results from ambient-noise surface-wave dispersion and from dip-corrected receiver functions. Our shear-velocity model reveals two significant findings. First, we identify a prominent fast-shear velocity anomaly at depths coinciding with the La Salle deformation belta north-south-trending fault-and-fold zone within the Illinois Basin. This anomaly may represent underplated mafic crust emplaced during rifting. Second, we observe a distinct shear-velocity boundary aligning approximately with the NW-trending Ste. Genevieve Fault Zone, a structure in Missouri that delineates part of the boundary between the Ozark Dome and the Illinois Basin and remains seismically active. Similar velocity boundaries have been attributed to the presence of steep crustal-penetrating faults, so the velocity boundary along the St. Genevieve fault suggests that the fault penetrates the crust to a depth of at least 50 km at a high angle. Faults with such geometry tend to initiate at transform faults, though they may alternatively have originated as steep normal faults in rifts. Overall, therefore, our shear-velocity model links shallow crustal structures and deeper crustal structures.

**S9-6** Machine learning for effective microseismicity monitoring: dataset, benchmarks, and adaptable models for carbon sequestration in Oklahoma. **Xiao, H.**, J. Walter (University of Oklahoma)

Induced earthquakes in the southern mid-continent of the United States present persistent monitoring challenges due to the low signal-to-noise ratios of small-magnitude events and historically relative sparse distribution of permanent stations distribution. Addressing these challenges requires both improved detection methods and adaptable solutions to diverse monitoring environments and equipment. We present a manually annotated seismic dataset from Oklahoma and surrounding regions (OK-

LAD, Oklahoma Labeled AI Dataset), spanning 2010-2025 and containing approximate 1.14 million traces. Most events are anthropogenic and fall within magnitudes 1.3 and depths of 48 km, making OKLAD a valuable resource for microseismic research and machine learning model development. Using OKLAD, we benchmarked and fine-tuned PhaseNet, EQTransformer and GPD frameworks. Our work demonstrated that minimum fine-tuning effectively improved detection performance for cataloged seismicity. We also explored adapting the models to real-world deployments: (1) configurations optimized for nodal deployments, enabling flexible and dense microseismic monitoring, and (2) downscaling strategies to even lighter architectures suitable for edge computing devices, opening potential for near-real-time, distributed detection. We present a robust dataset, model benchmarks, and adaptive workflow for Oklahoma. Together, these advances enhance capability of induced seismicity monitoring and provide important tools for potential carbon storage initiatives and related subsurface activities in Oklahoma.

**S8-12** Lessons Learned from Induced Earthquakes in the Southern Sichuan Basin, China. **Yang, H.**<sup>1</sup>, Jinping Zi<sup>2</sup>, Jiewen Zhang<sup>1</sup>, Aqeel Abbas<sup>2</sup>, and Yuyun Yang<sup>3</sup> (1: The Chinese University of Hong Kong; 2: SZRI, The Chinese University of Hong Kong; 3: Lingnan University)

Over the past two decades, shale gas development has flourished in many countries around the world. However, numerous shale gas fields have experienced successive earthquakes, making the effective control of seismic risks and ensuring safe production an urgent topic for in-depth research. The shale gas fields in southern Sichuan Province serve as a national comprehensive demonstration zone for shale gas development. Investigating the seismic mechanisms in this region is critically important for ensuring the safe and sustainable development of shale gas resources in China. Over recent years, we have conducted integrated research utilizing data from seismology, geodesy, and dense seismic array observations, applying a suite of

analytical methods. Our findings reveal the occurrence of extremely shallow earthquakes, challenging conventional assumptions about seismogenic depth. We also identified prolonged activation of a blind fault that ultimately ruptured during the damaging 2019 Mw 5.0 Weiyuan earthquake. In addition, our study uncovered novel mechanisms by which fluid injection can trigger seismic events, and highlighted distinct differences in stress drops between earthquakes occurring on major seismogenic faults and those near hydraulic fracturing zones. Notably, certain seismic waveforms exhibit signatures indicative of subsurface fluid activity, offering a promising new approach for mapping underground fluid distributions. These results not only advance our understanding of induced seismicity but also contribute to the broader field of earthquake source physics. Furthermore, our findings provide a critical scientific foundation for local authorities to develop regulatory frameworks aimed at mitigating seismic risks associated with shale gas development.

**S4-5** Evidence of lithospheric delamination below the North American midcontinent that ended subsidence in cratonic basins. **Yang, X.<sup>1</sup>, L. Peng<sup>2</sup>, A. L. Stevens Goddard<sup>3</sup>, L. Liu<sup>4</sup>** (1: Purdue University; 2: University of Illinois Urbana-Champaign; 3: Indiana University; 4: IGG, Chinese Academy of Sciences)

Cratonic lithospheres carry a long history of tectonic modifications that result in heterogeneous structures, as revealed by an increasing number of geophysical observations. The existence of cratonic basins indicates protracted periods of tectonic modification, causing subsidence within global continental interiors. An enigmatic aspect of this process is the cessation of subsidence in cratonic basins with unclear mechanisms. Here, using full-wave ambient noise tomography, we reveal distinct seismic low-velocity anomalies below 60 km beneath the Illinois and Michigan Basins, where subsidence terminated in the late Paleozoic to the early Mesozoic. These low-velocity volumes, surrounded by distinctly higher velocities, reflect the infiltrated

asthenospheric material that replaced the lithosphere lost during the delamination. This lithospheric modification may be associated with a major regional tectonic exhumation in the early Mesozoic that could have terminated basin subsidence and unroofed upper portions of basin stratigraphy. This timing coincides with the passage of this region over mantle plumes, which likely triggered lithospheric delamination and asthenospheric upwelling. Geodynamic modeling shows that the emplacement of these buoyant asthenospheric materials would lead to an uplift of about 3.5 km, sufficient to terminate the subsidence in the cratonic basins within this region. The findings of this study document lithospheric delamination in the North American midcontinent and present important links between geodynamic drivers and geological records of the evolution of the cratonic lithosphere in North America and beyond.

**S8-4** Estimation of Relative Magnitudes and Spectral Characteristics of Acoustic Emission Events during Granular Shear. **Zambrano, E., T. H. Goebel** (University of Memphis)

The characterization of acoustic emissions (AEs) in laboratory experiments is a fundamental tool to document strain energy accumulation and release in frictional media, and to bridge small-scale observations with earthquake source processes. In this work, we present preliminary results of acoustic events recorded during stick-slip tests in granular media between PMMA blocks. We compare magnitude distributions and source spectra between AEs in glass spheres and quartz sand. The recordings were acquired using a 12-channel array of high-frequency piezo-ceramic sensors, currently undergoing calibration. For this reason, the current analysis is performed in terms of relative amplitudes. To minimize sensor-to-sensor gain differences, peak amplitudes were normalized by a reference value from the same sensor (e.g., pre-event RMS). Relative magnitudes were then calculated for each sensor individually, and the resulting magnitudes were averaged across the 12-sensor array to obtain a representative magnitude per event.

This procedure reduces sensor-to-sensor variability and ensures consistent estimates across the full dataset. The methodologies applied include: (i) estimation of relative magnitudes and calculation of the frequency-magnitude distribution (FMD); and (ii) spectral analysis, exploring the variation in the frequency content and the relationship between relative magnitude and corner frequency. We test whether there are scaling trends in the laboratory that are consistent with earthquake source relations observed for tectonic seismicity. Preliminary results suggest

that relative magnitudes allow us to observe general trends in energy release and event size distribution. In addition, first-order spectral differences between events of varying size indicate that relative magnitude can provide meaningful insight into the scale of acoustic emissions. This methodological framework lays the groundwork for future studies with fully calibrated AEs sensors, enabling the derivation of source parameters such as seismic moment in physical units for a comparison with larger-scale seismicity.